Contents

Chapter 1

Introduction

dfdf [6]

Chapter 2

Distillation control (will place this in other chapters)

2.1 optimal operation

With an objective function defined, we solve an optimization problem to find the optimal operating point

$$\min_{\mathbf{x},\mathbf{u}} J(\mathbf{x},\mathbf{u},\mathbf{d}) \tag{2.1}$$

subject to

$$\begin{aligned} \mathbf{f}(\mathbf{x},\mathbf{u},\mathbf{d}) &= 0 \\ \mathbf{g}(\mathbf{x},\mathbf{u},\mathbf{d}) &\leq 0 \\ \mathbf{y} &= \mathbf{f}_{\mathbf{y}}(\mathbf{x},\mathbf{u},\mathbf{d}) \end{aligned} \tag{2.2}$$

where $\mathbf{x}$ is the vector of internal variables (states), $\mathbf{u}$ are the manipulated variables (inputs) and $\mathbf{d}$ is the vector of disturbances. $\mathbf{f}$ are typically the model equations and the inequality constraints $\mathbf{g}$ are process constraints such as process limitations or safety constraints. $\mathbf{y}$ is the vector of measurements.

2.2 self-optimizing control

2.3 singular value method

2.3.1 Minimum singular value rule

In this work we make use of the Singular Value Rule of Halvorsen to find the best temperatures to control in each case. The procedure is summarized here. 1. Using a linear model we scale the inputs u_j such that a unit deviation in each input has the same effect on the cost function J. $u_{scl,j} = 1/\sqrt{[J_{uu}]_{jj}}$. 2. For each candidate controlled variable, we obtain its optimal variation due to disturbances v_i. Assuming the setpoints are nominally optimal, $v_i = [GJ_{uu}^{-1}J_{ud} - G_d]d$. 3. For each candidate controlled variable, we obtain its expected implementation error n_i (sum of measurement error and control error). 4. Using the sum of the magnitudes of v_i and n_i (often called "span"), we scale the candidate controlled variables. $c_{scl,i} = |v_i| + |n_i|$. 5. We then compute the scaling matrices, $D_c = diag\{c_{scl,i}\}$, and $D_u = diag\{u_{scl,j}\}$ and obtain the scaled model $G' = D_c^{-1}GD_u$. 6. Finally, we select as candidates those sets of controlled variables that correspond to a large value of the minimum singular value $\underline{\sigma}(G')$.

Note on input scaling

In the above method it is assumed that J_{uu} can be described as a constant times a unitary matrix. However, this is not always appropriate, and we shall see in the following results that this assumption can lead to suboptimal sets of controlled variables. An alternative is to make use of the full J_{uu}, giving $u_{scl,jj} = 1/\sqrt{[J_{uu}]_{jj}}$.

2.4 null-space method

2.5 Selection of secondary controlled variables

*

pair close

large gain - steep slope

maximum gain rule

*Note to self, not part of thesis: general requirements. methods

Chapter 3

Dividing wall distillation

Chapter 4

Kaibel column model

Chapter 5

Optimal Operation of the Kaibel Column

To define optimal operation we must decide what the objectives of the operation are. Usually the operation is to perfom a certain task with some specifications on quantity and quality. To find optimal operation, we can measure the performance according to our defined criterion, which generally is to maximise profit subject to satisfying given constraints and specifications. Depending on the situation, this can be translated to more specific objectives such as maximize throughput, maximize quality (purity), minimize energy, minimize time etc.

5.1 Top-down analysis

We define a general economic objective function, namely to minimize the cost J:

$$(-J) = \sum_{i=1}^{m} P_{pi} P_i - \sum_{j=1}^{n} P_{fj} F_j - \sum_{k=1}^{o} P_{ek} E_k \tag{5.1}$$

where P_p, P_f, and P_e denote the prices of products, feedstocks and energy respectively.

The optimization problem then becomes:

$$\min_{\mathbf{u}} J \tag{5.2}$$

subject to

$$\begin{aligned} \mathbf{f}(\mathbf{x}, \mathbf{u}, \mathbf{d}) &= 0 \\ \mathbf{h}(\mathbf{x}) &\leq 0 \end{aligned} \tag{5.3}$$

where $\mathbf{f} = 0$ expresses the model equations and the equality constraints and $\mathbf{h} \leq 0$ the inequality constraints.

5.2 Modes of operation

The performance objective to minimize the cost in Eq. 5.1 is typical in considering the operation of a whole plant, and to include the all aspects of the economic performance, additional terms and parameters would probably be included. But, we can also apply the idea of optimal operation on a single unit such as a distillation column. The operational objective of a distillation column is largely dependent on its role in the plant (process). The task of a column could be to remove small amounts of undesireable components from a feedstock, providing a rough separation of petrochemicals before further separation or to produce high purity products as the last major process unit in the plant. The definition of an objective function for optimal operation thus depends on the purpose of the unit.

Below we give four different examples of the operation of a Kaibel distillation column, depending on the task given to the column. The purpose of this is to illustrate the procedures of a plantwide control approach (Chapter 2) and further on we shall see that the operational objective has a large influence on the controlled variables used to achieve optimal operation.

5.2.1 Case 1. Maximize purity

It is quite common, from an economical perspective if energy is relatively cheap, that it is optimal to maximize the purity of all the product streams from a distillation column, or equivalently to minimize the sum of its impurities:

$$J = \sum impurities = \sum P_i(1 - x_{i,P_i}) \tag{5.4}$$

Where i denotes both the product number and the main component in this product. In the simplest case, we minimize the sum of impurities with no weighting included. This would apply if the main component in all products are of equal value and there is no income from impurities.

For this case, we make the following main assumptions:

Given feed, F. The feed to the column is assumed given by an upstream process or set at a constant rate. The feed rate will be included in the disturbance vector in the following analysis.

Given boil up, $V = V_{max}$. We assume that heat input to the column and hence boil up is set at a constant rate. If energy is relatively

cheap, it is optimal to set it at the maximum allowable as this will minimize the amount of impurities in the product streams.

For a case with four main components (A,B,C,D) and two side streams the cost function then becomes:

$$\begin{aligned} \min_{u_0} J &= D(1-x_{A,D}) + S_1(1-x_{B,S_1}) \\ &\quad + S_2(1-x_{C,S_2}) + B(1-x_{D,B}) \end{aligned} \tag{5.5}$$

Degrees of freedom - active constraints

In this case, F and V are treated as active constraints and we are left with 5 unconstrained degrees of freedom for optimization: $\mathbf{u^T} = [L\ S_1\ S_2\ R_L\ R_V]$

5.2.2 Case 2: minimize energy usage

One of the great benefits of the Kaibel column is the potential for energy savings compared with separation in a series of columns, and will perhaps in the future be the principial reason for installing such a column. Thus, an operator having installed a Kaibel column may want to take full advantage of the reduced energy cost of operation and for a given product specification, minimize energy input to the column.

In the following, we relate energy usage to the vapor boil up, V, and the optimization problem can be formulated as follows, again with the feedrate set:

$$\min_{\mathbf{u}} J = V \tag{5.6}$$

given feed, F.

where in the constraints $\mathbf{h}$ of Equation 5.3 are included the product specifications, which are here selected to be:

$$\begin{bmatrix} x_{A,D} \\ x_{B,S_1} \\ x_{C,S_2} \\ x_{D,B} \end{bmatrix} \geq \begin{bmatrix} 0.975 \\ 0.94 \\ 0.94 \\ 0.975 \end{bmatrix}$$

Degrees of freedom - active constraints

Assuming the four product specifications are active, we need to use 4 inputs to control these acitve constraints. We are then left with 2 inputs for optimization (minimizing the energy usage in (5.6): $\mathbf{u^T} = [R_L\ R_V]$

Comment : One would expect that the purity constraints are all active, as "overpurification" costs energy. However, as shown by Alstad [1,] this is not always the case in a Petlyuk column because overpurification may be achieved "for free" because the column may be "unbalanced". Nevertheless, the possible energy savings by overpurifications are small, so we here assume that all purity constraints are active.

5.2.3 Case 3: maximum profit with uneven pricing

In this scenario, two of the products are more valuable than the other two. An industrial example could be the separation of iso-pentane (A), n-pentane (B), iso-hexane (C) and n-hexane (D), where the iso-alkanes (A and C) are the more valuable as octane boosters. In our case we use the components A,B,C,D and we set the product values according to table 5.1 (The components are modelled as Methanol, Ethanol,n-Propanol and n-Butanol). In the distillate and sidestream 2, the price is paid for the main component only (so the impurity have zero value), while in the first sidestream and bottoms product the price is the same for all components.

Table 5.1: Product values

Product stream	Value ($/t)	Component
Distillate	200	A
Sidestream 1	150	Any (sold as fuel)
Sidestream 2	200	C
Bottoms	150	Any (sold as fuel)
Feed	150	

Again, we fix the vapour boil-up rate and the optimal operation problem can be stated as:

$$\min_{\mathbf{u_0}} J = -\Big(\dot{m}_{A,D}P_D + \sum_{i=1}^{n}\dot{m}_{i,S_1}P_{S_1} + \dot{m}_{C,S_2}P_{S_2} + \sum_{i=1}^{n}\dot{m}_{i,B}P_B\Big) \qquad (5.7)$$

subject to

given feed. F

given boil up, $V = V_{max}$.

Degrees of freedom - active constraints

The degrees of freedom are here the same as in the maximum purity case (section 5.2.1). We have two constrained degrees of freedom (F, V) and five unconstrained:
$\mathbf{u^T} = [L\ S_1\ S_2\ R_L\ R_V]$

5.2.4 Case 4: maximum throughput

In most cases, the prices are such that profit increases when the feedrate increases (allthough the profit pr. kg may drop because the efficiency drops). Thus, if feed is available and there is a market for the products, maximizing the throughput will lead to maximized profit. For a distillation column, this can be translated into maximizing the feed flowrate, F. When maximizing throughput of a process, there will be one or more limiting factors (bottlenecks), typically depending on equipment size, utility loads etc. In our case we define a set of product specifications and assume that the vapour boil-up, V, will be the limiting bottleneck. Thus,

$$\min_{\mathbf{u_0}} J = -F \tag{5.8}$$

subject to

given purity specifications, $x_i \geq x_{i,spec}$.

given boil up, $V = V_{max}$.

Degrees of freedom - active constraints

Assuming that the 4 product specifications are active, we are then left with two unconstrained degrees of freedom. For example R_V may be used in addition to F:
$\mathbf{u^T} = [F\ R_V]$.

5.2.5 Discussion

Table 5.2 show the

Table 5.2: Overview of operational modes. Number of unconstrained degrees of freedom in each case and the corresponding nominal optimal input values. The values of the constrained variables are shown in bold.

	Case 1	Case 2	Case 3	Case 4
No. of unconstr. DOF's	5	2	5	2
Optimal inputs				
F	**1.0000**	**1.0000**	**1.0000**	1.0708
L	2.8492	2.6537	2.8594	2.8416
V	**3.0000**	2.8017	**3.0000**	**3.0000**
S_1	0.2494	0.2437	0.2681	0.2609
S_2	0.2497	0.2523	0.2396	0.2702
R_L	0.2572	0.2353	0.2642	0.2353
R_V	0.3770	0.3611	0.3850	0.3611
D	0.2508	0.2480	0.2406	0.2655
B	0.2501	0.2560	0.2518	0.2741
Nominal purities				
$x_{A,D}$	0.9703	**0.9750**	0.9830	**0.9750**
x_{B,S_1}	0.9361	**0.9400**	0.8946	**0.9400**
x_{C,S_2}	0.9589	**0.9400**	0.9737	**0.9400**
$x_{D,B}$	0.9949	**0.9750**	0.9900	**0.9750**

Chapter 6

Supervisory control

6.1 Selecting controlled outputs

In applying the steps of the top-down analysis outlined in chapter 2, we now want to select the primary controlled variables.

Control active constraints

To achieve optimal operation, the active constraints should be controlled at their constraint values.

Controlled variables associated with unconstrained degrees of freedom

If, after controlling the active constraints, there are remaining unconstrained degrees of freedom, then we need to find a control policy for how they should be used. Generally, we want to control combinations of measurements at constant setpoints. This is known as "self-optimizing" control. Here we use the extended null-space method of Alstad (ref!!!!) outlined in Chapter 2.

With the active constraint loops closed (including loops on top and bottom levels using D and B), the model is linearized around the nominal optimal point to yield

$$\Delta \mathbf{y}_0 = \mathbf{G}^{y_0} \Delta \mathbf{u} + \mathbf{G}_d^{y_0} \Delta \mathbf{d} \tag{6.1}$$

where $\mathbf{u}$ denotes the remaining unconstrained degrees of freedom, $\mathbf{y_0}$ the available measurements are the temperatures of each stage including the reboiler. The unconstrained degrees of freedom $\mathbf{u}$ vary depending on the case. The disturbances $\mathbf{d}$ generally include the feed conditions and the active constraints.

6.1.1 Case 1

6.1.2 Case 2

In the case where we want to minimize the energy usage subject to quality constraints on the product purities we found that we were left with two degrees of freedom after controlling the active constraints. For control of active constraints, we may use reflux, L, for controlling the distillate purity, $x_{A,D}$, and the vapor rate, V, to control the bottoms purity, $x_{D,B}$. The sidestream purities, x_{B,S_1} and x_{C,S_2} may be paired with the sidestream rates S_1 and S_2 respectively. The remaining unconstrained degrees of freedom are then the split ratios R_L and R_V, and the objective is to find some combinations of variables (measurements) to control at constant setpoints that will keep the process close to optimal operation (with acceptable loss) despite disturbances and implementation error. The following procedure was used:

Step 1. Optimization

The optimization problem in equation 5.6 was solved to find the optimal nominal operating point. The resulting value of the objective function was $V = 2.8017$, and the optimal input values can be seen in Table 5.2.

Step 2. Identification of variables

The linearized model of Equation 6.1 for this case have, as mentioned, the split ratios for inputs, while in the disturbance vector we have included the feed rate (F), feed compositions (z_i), the feed enthalpy (q) as well as the product specifications (active constraints).

$$\mathbf{u} = \begin{bmatrix} R_L \\ R_V \end{bmatrix} \tag{6.2}$$

$$\mathbf{d}^T = \begin{bmatrix} F & z_A & z_B & z_C & q & n_{x_{A,D}} & n_{x_{B,S_1}} & n_{x_{C,S_2}} & n_{x_{D,B}} \end{bmatrix} \tag{6.3}$$

$$\mathbf{y}_0 = \begin{bmatrix} T_1 \\ T_2 \\ \vdots \\ T_{65} \end{bmatrix} \tag{6.4}$$

Step 3. Scaling of variables

Each measurement is scaled with its corresponding implementation error ($|n_{y_{0,i}}|$). In this case all the measurements are temperatures, and they are given the same error of 0.5 K.

Each disturbance is scaled with its corresponding expected disturbance ($|\Delta d_{k,max}|$). In this example the feed rate and feed enthapy are given a 10% maximum expected disturbance and 5 % for the feed compositions.

The inputs are scaled using the Hessian matrix $\mathbf{J_{uu}}$. *

We then have the following scaling matrices

$$\mathbf{W_n^{y_0}} = \begin{bmatrix} |n_{y_{0,1}}| & & \\ & \ddots & \\ & & |n_{y_{0,n_{y_0}}}| \end{bmatrix} \mathbf{W_d} = \begin{bmatrix} |\Delta d_{1,max}| & & \\ & \ddots & \\ & & |\Delta d_{n_d,max}| \end{bmatrix} \tag{6.5}$$

Step 4. Selection of measurements

First we find the best subset of measurements using just enough measurements ($n_y = n_u + n_d = 2+9 = 11$). We use direct selection from all combinations that maximize the minimum singular value of the scaled augemented process model $\tilde{\mathbf{G}}^{y_0}$.

A branch and bound search give the following measurements†:

$$\mathbf{y^T} = \begin{matrix} [T_7 & T_{12} & T_{18} & T_{21} & T_{24} \\ T_{28} & T_{36} & T_{37} & T_{47} & T_{49} & T_{60}] \end{matrix} \tag{6.6}$$

The location of the measurements in the column can be seen in Figure ‡

Step 5. Null space method

Next, using the explicit expression for the optimal $\mathbf{H}$ for combined disturbances and measurement errors we find the linear combination of the measurements to form the self-optimizing controlled variables. (Scaled using the largest element)

*Note to self, not part of thesis: MORE HERE.

†This is a very demanding computation as there are 8.95×10^{12} possible combinations

‡Note to self, not part of thesis: MAKE FIGURE.

Table 6.1: Disturbance loss

disturbance	magnitude	%-loss
ΔF	$+10\%$	0.0
ΔF	-10%	0.0
$\Delta z_{A,F}$	$+5\%$	0.0086
$\Delta z_{A,F}$	-5%	0.0107
$\Delta z_{B,F}$	$+5\%$	0.0058
$\Delta z_{B,F}$	-5%	0.0065
$\Delta z_{C,F}$	$+5\%$	0.0079
$\Delta z_{C,F}$	-5%	0.0028
Δq	$+10\%$	0.0254
Δq	-10%	0.0218

$$\begin{aligned} c_{soc,1} &= -T_7 + 0.073T_{12} + 0.405T_{18} - 0.707T_{21} + 0.034T_{24} - 0.147T_{28} \\ &\quad +0.369T_{36} + 0.257T_{37} - 0.030T_{47} + 0.236T_{49} + 0.553T_{60} \end{aligned} \quad (6.7)$$

$$\begin{aligned} c_{soc,2} &= T_7 - 0.073T_{12} - 0.405T_{18} + 0.707T_{21} - 0.034T_{24} + 0.147T_{28} \\ &\quad -0.369T_{36} - 0.257T_{37} + 0.030T_{47} - 0.236T_{49} - 0.553T_{60} \end{aligned} \quad (6.8)$$

Loss calculations

Keeping $c_{soc,1}$ and $c_{soc,2}$ constant the worst case loss ($L_{wc} = \frac{1}{2}(\overline{\sigma}\,[\mathbf{M}])^2$) comes out as 0.0068. This can be compared with the loss when we include all available measurements, which is $L_{wc}^{all} = 1.9 \times 10^{-5}$

Loss using nonlinear model

* The loss in the objective function when disturbances are introduced using the nonlinear model can be seen in table 6.1

6.1.3 Case 3

*Note to self, not part of thesis: Show results

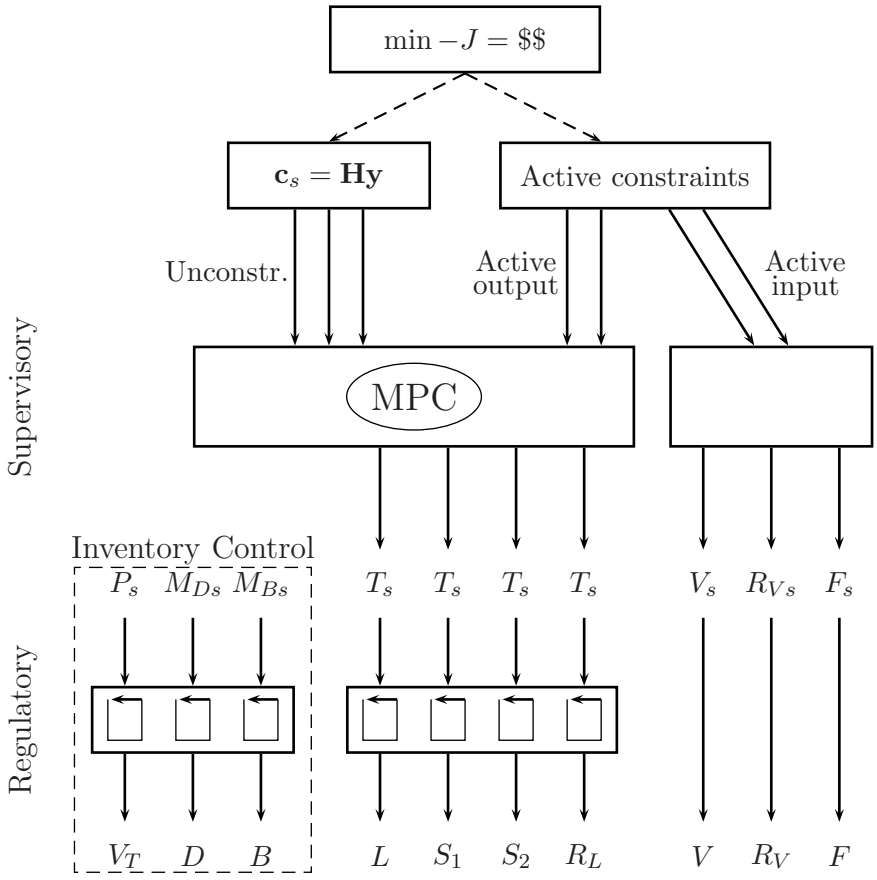

Figure 6.1: Control hierarchy

Chapter 7

Practical control of dividing-wall columns

7.1 Introduction

This chapter introduces some more practical aspects of how to go about operating a dividing-wall column. While in the previous chapter we defined the steady-state optimal operation, we will here focus on how to operate the column in practice, where the goal is to achieve acceptable operation using simple control policies.

In particular, we will investigate the importance of properly adjusting the liquid split ratio, R_L, which determines the relative amount of reflux to the two sides of the dividing wall.

Furthermore, we would like to compare the same analysis on both the Kaibel column and on a Petlyuk column. Are there any inherent differences in the operation of these two types of dividing wall column?

The example used is taken from Section 5.2.1 where the overall objective (Equation 7.1) is to minimize the sum of the impurity flows of all product streams.

$$\begin{aligned} J &= D(1 - x_{A,D}) + S_1(1 - x_{B,S_1}) \\ &\quad + S_2(1 - x_{C,S_2}) + B(1 - x_{D,B}) \end{aligned} \tag{7.1}$$

We assume fixed feed rate (F), fixed vapor boilup rate ($V = V_{max}$) and fixed vapor split ratio (R_V). Assuming that the distillate (D) and bottoms (B) flows are used for level control, the remaining degrees of freedom for control are then the reflux (L), the side stream flows (S_1 and S_2) and the liquid split ratio (R_L).

These remaining four degrees of freedom are sometimes held constant, but preferably they should be adjusted during operation, for example, by keeping selected temperatures constant. Three cases are studied in the paper.

1. One temperature loop: Reflux,L is used for temperature control (Also used for the other cases
2. Three temperature loops: Adding temperature loops for the two side streams (S_1 and S_2)
3. Four temperature loops: Adding a temperature loop for the liquid split, R_L

The three different control configurations are indicated in Figure 7.2, where the location of the temperature measurements are also indicated. The locations were chosen without a detailed analysis, based on dynamic consideration and common recommendations. *

Loss definitions

Throughout this chapter we compare the resulting objective function value (impurity flows) after changes in the inputs (J_d) relative to the nominal (optimal) value (J_{nom}):

$$L_{nom} = \frac{J_d - J_{nom}}{J_{nom}} \tag{7.2}$$

For disturbances, we also define the loss relatice to the truly optimal J for the given disturbance, $J_{opt,d}$ (reoptimized with respect to L, S_1, S_2 and R_L):

$$L_{opt} = \frac{J_d - J_{opt,d}}{J_{opt,d}} \tag{7.3}$$

7.2 Kaibel Column

7.2.1 Effect of liquid split ratio

The nominal operating point for the Kaibel column is taken from Chapter 5. We first investigate how the column behaves for the two cases when the liquid split ratio is kept constant and not used for control. Starting from the nominal point we have the first case where only one temperature loop is closed using the reflux, L (Figure 7.2a). The second case is where

*Note to self, not part of thesis: add references

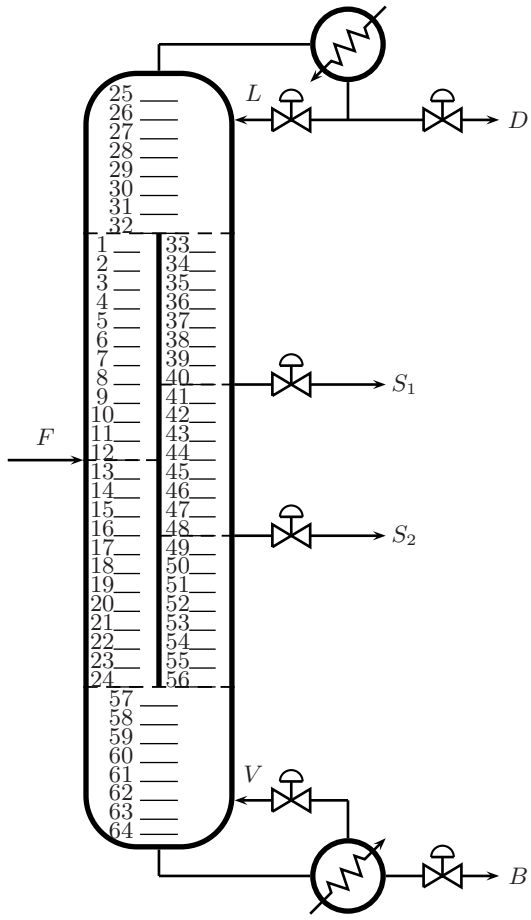

Figure 7.1: Kaibel dividing-wall column. Stage numbering

Table 7.1: Kaibel column with one temperature loop closed: Effect of changes in R_L

	$\Delta R_{L,-50}$	$\Delta R_{L,-25}$	Nominal	$\Delta R_{L,+25}$	$\Delta R_{L,+50}$
R_L	**0.1286**	**0.1929**	**0.2572**	**0.3215**	**0.3858**
F	1.0000	1.0000	1.0000	1.0000	1.0000
$z_{i,F}$	0.2500	0.2500	0.2500	0.2500	0.2500
V	3.0000	3.0000	3.0000	3.0000	3.0000
R_V	0.3770	0.3770	0.3770	0.3770	0.3770
L	2.8547	2.8525	2.8492	2.8457	2.8502
$S1$	0.2494	0.2494	0.2494	0.2494	0.2494
$S2$	0.2497	0.2497	0.2497	0.2497	0.2497
D	0.2453	0.2475	0.2508	0.2543	0.2498
B	0.2556	0.2534	0.2501	0.2466	0.2511
$x_{A,D}$	0.9759	0.9733	0.9703	0.9701	0.9704
x_{B,S_1}	0.7166	0.8223	0.9361	0.8788	0.8055
x_{C,S_2}	0.7163	0.8455	0.9589	0.8907	0.8208
$x_{D,B}$	0.9406	0.9855	0.9949	0.9977	0.9918
J	0.1626	0.0932	0.0349	0.0657	0.1027
L_{nom} (%)	366	167	0	88	194

we have three temperature loops closed, using S_1 and S_2 in addition to L (Figure 7.2b). The setpoints for the temperature controllers are kept at their nominal values, while we vary the liquid split ratio R_L away from its optimal value.

We set $R_L = 0.50R_{L,opt}$ and $R_L = 0.75R_{L,opt}$, which signifies that more (too much) reflux is directed to the main column. Also, we increase R_L by 25 and 50% , which means that more reflux is directed to the prefractionator as compared to the optimal value.

Input values, resulting product purities, objective function value and percentage loss for the case with one temperature loop can be seen in Table 7.1 and Table 7.2 shows the values for the case with three temperature loops closed.

From the tables we see that changing the liquid split away from its optimal setting has a detrimental effect on the side stream purities. The configuration with three temperature loops performs slightly better than the one-loop configuration, but the differences are relatively small. For the largest positive change in R_L, the three-loop configuration is actually the worst. This is because the controller on sidestream 2 enforces a large flow on the stream with most impurities.

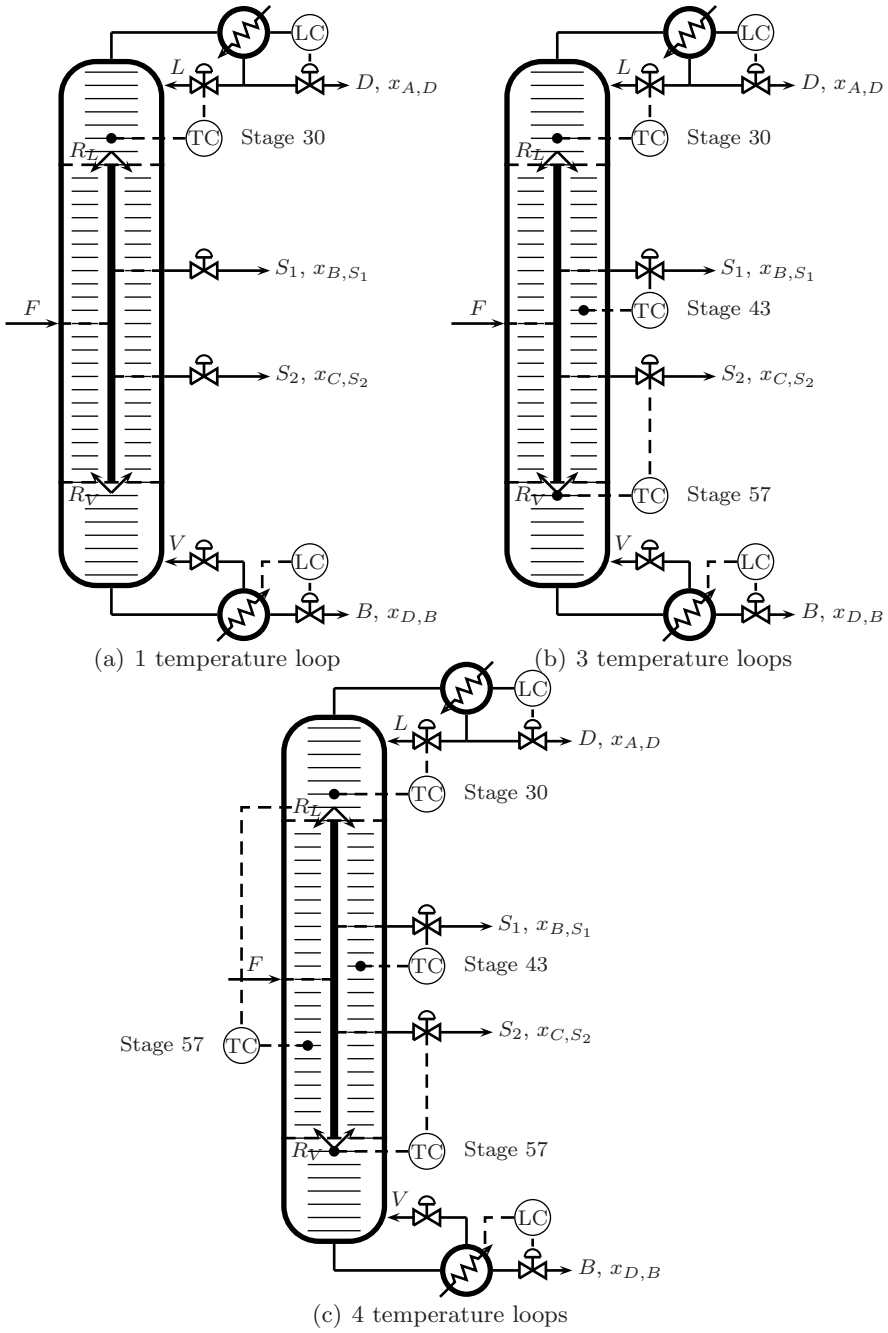

(a) 1 temperature loop

(b) 3 temperature loops

(c) 4 temperature loops

Figure 7.2: Kaibel column control configurations (In all cases F, V and R_V are fixed)

Table 7.2: Kaibel column with 3 temperature loops closed: Effect of changes in R_L

	$\Delta R_{L,-50}$	$\Delta R_{L,-25}$	Nominal	$\Delta R_{L,+25}$	$\Delta R_{L,+50}$
R_L	**0.1286**	**0.1929**	**0.2572**	**0.3215**	**0.3858**
F	1.0000	1.0000	1.0000	1.0000	1.0000
$z_{i,F}$	0.2500	0.2500	0.2500	0.2500	0.2500
V	3.0000	3.0000	3.0000	3.0000	3.0000
R_V	0.3770	0.3770	0.3770	0.3770	0.3770
L	2.8559	2.8533	2.8492	2.8455	2.8499
$S1$	0.2880	0.2812	0.2494	0.2234	0.1996
$S2$	0.2268	0.2213	0.2497	0.2741	0.3221
D	0.2441	0.2467	0.2508	0.2545	0.2501
B	0.2411	0.2508	0.2501	0.2480	0.2282
$x_{A,D}$	0.9760	0.9734	0.9703	0.9701	0.9703
x_{B,S_1}	0.7141	0.8109	0.9361	0.9388	0.9105
x_{C,S_2}	0.8071	0.9283	0.9589	0.8701	0.7339
$x_{D,B}$	0.9950	0.9949	0.9949	0.9971	0.9985
J	0.1332	0.0769	0.0349	0.0576	0.1113
L_{nom} (%)	282	120	0	65	219

Figure 7.3 shows the temperature profiles in the column for the case with 3 temperature loops. The first (a) is the nominal (optimal) operating point, while the second (b) and third (c) show the profiles when the liquid split is set too low ($0.50R_{L,opt}$) and too high ($1.50R_{L,opt}$) respectively. The three controlled temperatures are all in the main column (as indicated in the figure), so that when more of the reflux is directed to the main column (b), the prefractionator temperature profile is shifted upwards, while the main column profile has less shift . Conversely, when too much reflux is sent to the prefractionator (c), the section is cooled and the profile is "lowered".

The corresponding compostition profiles of the prefractionator and main column are shown in Figure 7.4. The effect of an incorrectly set liquid split ratio is readily observed here. When R_L is too low, we can observe a breakthrough of component C in from the top of the prefractionator into the main column (Fig 7.4c). This leads in turn to large impurity in the first sidestream (Fig. 7.4d). Figure 7.4 e) and f) show the composition profiles when R_L is set too high. Here we get breaktrough of component B from the bottom of the prefractionator into the main column. This prevents us from reaching high purity in the second sidestream.

In both the cases where the liquid split ratio is implemented incorrectly

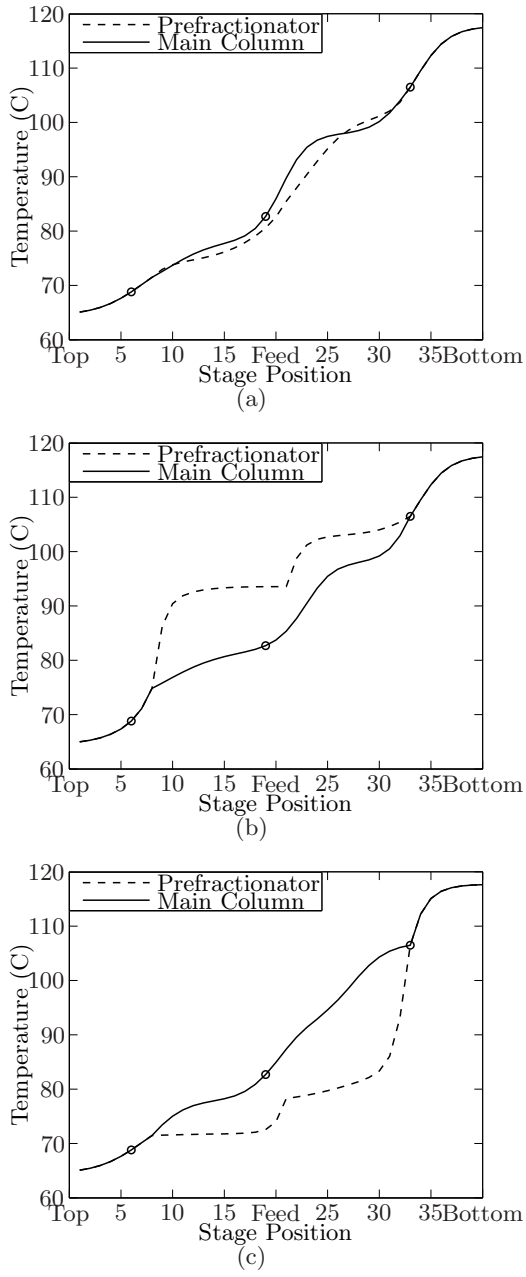

Figure 7.3: Kaibel column with 3 temperature loops closed: Column temperature profiles. (a) Nominal profile, (b) $R_L = 0.50R_{L,opt}$, (c) $R_L = 1.50R_{L,opt}$. Controlled temperatures are circled.

Table 7.3: Kaibel column: Optimal operating point for disturbances R_V fixed

	ΔF_{+10}	$\Delta z_{B,F,+20}$	$\Delta R_{V,+10}$	$\Delta R_{V,+50}$
F	1.1000	1.0000	1.0000	1.0000
$z_{i,F}$	0.2500	0.3000	0.2500	0.2500
V	3.0000	3.0000	3.0000	3.0000
R_L	0.2443	0.2386	0.2967	0.4552
R_V	0.3770	0.3770	0.4147	0.5655
L	2.8340	2.8491	2.8491	2.8486
S_1	0.2745	0.3004	0.2493	0.2484
S_2	0.2745	0.2489	0.2498	0.2506
D	0.2760	0.2509	0.2509	0.2514
B	0.1750	0.1997	0.2500	0.2496
$x_{A,D}$	0.9680	0.9645	0.9692	0.9630
x_{B,S_1}	0.9329	0.9369	0.9364	0.9352
x_{C,S_2}	0.9579	0.9567	0.9593	0.9590
$x_{D,B}$	0.9946	0.9955	0.9949	0.9943
$J_{opt,d}$	0.0403	0.0395	0.0350	0.0371

we observe large reductions in the sidestream product purities (*cf.* Loss in Table 7.2). Clearly, it is important to achieve the right split of the reflux for the successful operation of the Kaibel column.

Before we look into how to adjust the liquid split ratio, we will see how the single-loop and 3-loop configurations perform under some different disturbances.

7.2.2 Disturbance rejection

The two control configurations (1-loop and 3-loop) are subjected to disturbances in feedrate (F), feed composition (z_F) and vapor split (R_V). The disturbance in feed composition is a 20 % increase in $z_{B,F}$ with corresponding reduction in $z_{D,F}$. For the vapor split, both a 10 % and a 50 % increase is simulated. To compare the results of the simulations, we have reoptimized the solution with respect to L, S_1, S_2 and R_L for each disturbance with R_V fixed. The optimal values can be seen in Table 7.3.

Tables 7.5 and 7.6 show the relevant inputs, resulting purities and objective function values after the disturbances for the two configurations. Here, the three-loop configuration is clearly better than the case with only one temperature loop as can be expected. However, the large change in vapor split (R_V) cannot be handled by either configuration.

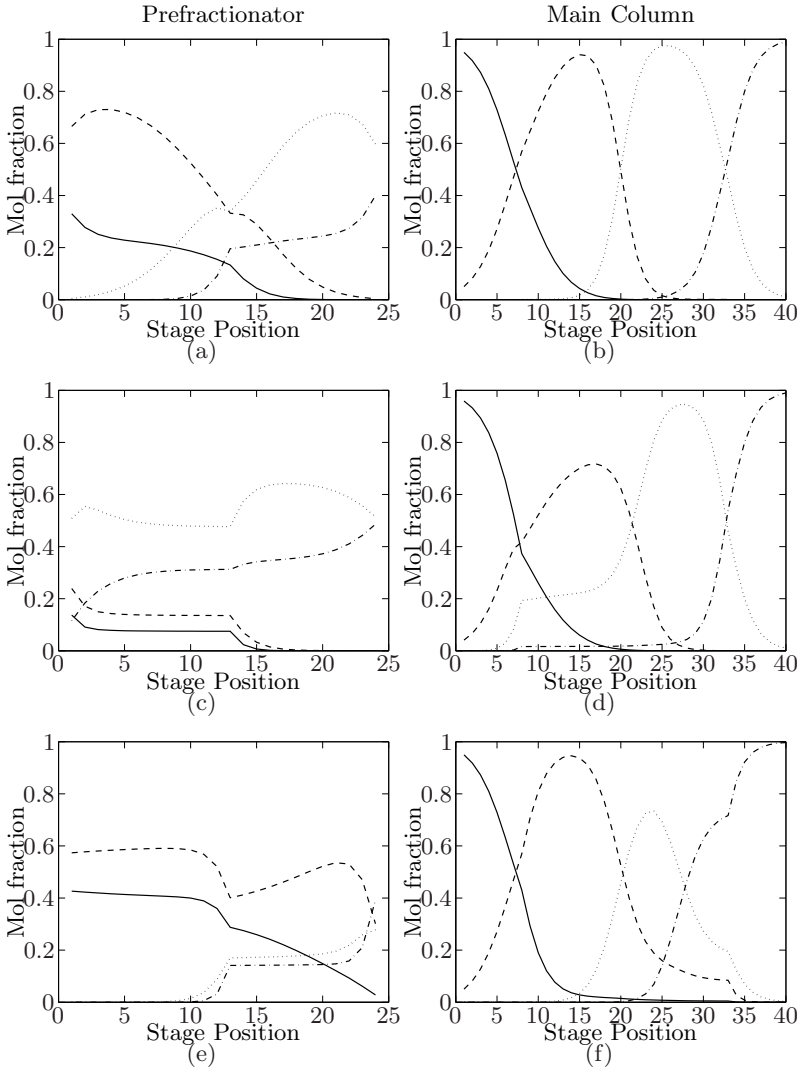

Figure 7.4: Kaibel column with 3 temperature loops closed: Composition profiles of prefractionator and main column. (a) and (b) nominal operating point, (c) and (d) R_L is too low, (e) and (f) R_L is too high. (—— component A, − − − component B, · · · component C, − · − component D)

Table 7.4: Kaibel column: Optimal operating point for disturbances R_L and R_V fixed

	Nominal	ΔF_{+10}	$\Delta z_{B,F,+20}$	$\Delta R_{V,+10}$
F	1.0000	1.1000	1.0000	1.0000
$z_{i,F}$	0.2500	0.2500	0.3000	0.2500
V	3.0000	3.0000	3.0000	3.0000
R_L	0.2572	0.2572	0.2572	0.2572
R_V	0.3770	0.3770	0.3770	0.4147
L	2.8492	2.8339	2.8485	2.8500
S_1	0.2494	0.2703	0.2943	0.2726
S_2	0.2497	0.2787	0.2531	0.2274
D	0.2508	0.2761	0.2515	0.2500
B	0.2501	0.1750	0.2011	0.2501
$x_{A,D}$	0.9703	0.9703	0.9670	0.9679
x_{B,S_1}	0.9361	0.9349	0.9402	0.8504
x_{C,S_2}	0.9589	0.9439	0.9381	0.9514
$x_{D,B}$	0.9949	0.9946	0.9915	0.9963
J	0.0349	0.0429	0.0433	0.0608

The dynamic responses for the case with three temperature loops are shown in Figure 7.5.

7.3 Using liquid split for feedback control

So far we been keeping the liquid split ratio (R_L) constant, while using the reflux and side stream flows to control selected temperatures. However, the liquid split is also a degree of freedom that can be used for control. We will now add an additional temperature using R_L to the Kaibel dividing-wall column, and compare the perfomance to the previous configurations.

7.3.1 Kaibel column with four temperature loops

The fourth temperature loop is added to "stabilize" the prefractionator profile using the liquid split as manipulated variable. The temperature selected should be in the prefractionator section of the column, and the particular stage location used here was chosen considering the steady-state gain and the stage-to-stage temperature difference, but no detailed analysis was made.

With four temperature loops now closed, we subject the model to the

Table 7.5: Kaibel column with 1 temperature loop closed: Effect of disturbances

	Nominal	ΔF_{+10}	$\Delta z_{B,F,+20}$	$\Delta R_{V,+10}$	$\Delta R_{V,+50}$
F	1.0000	1.1000	1.0000	1.0000	1.0000
$z_{B,F}$	0.2500	0.2500	0.3000	0.2500	0.2500
V	3.0000	3.0000	3.0000	3.0000	3.0000
R_L	0.2572	0.2572	0.2572	0.2572	0.2572
R_V	0.3770	0.3770	0.3770	0.4147	0.5655
L	2.8492	2.8330	2.8493	2.8520	2.8764
$S1$	0.2494	0.2494	0.2494	0.2494	0.2494
$S2$	0.2497	0.2497	0.2497	0.2497	0.2497
D	0.2508	0.2770	0.2507	0.2480	0.2236
B	0.2501	0.3239	0.2502	0.2529	0.2773
$x_{A,D}$	0.9703	0.9692	0.9703	0.9723	0.9813
x_{B,S_1}	0.9361	0.9586	0.9658	0.8642	0.4993
x_{C,S_2}	0.9589	0.8896	0.7925	0.8883	0.4963
$x_{D,B}$	0.9949	0.8485	0.7989	0.9875	0.8820
J	0.0349	0.0955	0.1181	0.0718	0.2876
L_{nom} (%)	-	174	238	106	724
L_{opt} (%)	-	137	199	105	675

Table 7.6: Kaibel column with 3 temperature loops closed: Effect of disturbances

	Nominal	ΔF_{+10}	$\Delta z_{B,F,+20}$	$\Delta R_{V,+10}$	$\Delta R_{V,+50}$
F	1.0000	1.1000	1.0000	1.0000	1.0000
$z_{B,F}$	0.2500	0.2500	0.3000	0.2500	0.2500
V	3.0000	3.0000	3.0000	3.0000	3.0000
R_L	0.2572	0.2572	0.2572	0.2572	0.2572
R_V	0.3770	0.3770	0.3770	0.4147	0.5655
L	2.8492	2.8492	2.8502	2.8502	2.8636
$S1$	0.2494	0.2494	0.2968	0.2968	0.0705
$S2$	0.2497	0.2497	0.2541	0.2541	0.4483
D	0.2508	0.2508	0.2498	0.2498	0.2364
B	0.2501	0.2501	0.1994	0.1994	0.2447
$x_{A,D}$	0.9703	0.9692	0.9704	0.9723	0.9812
x_{B,S_1}	0.9361	0.9364	0.9363	0.8510	0.4594
x_{C,S_2}	0.9589	0.9426	0.9362	0.9444	0.4963
$x_{D,B}$	0.9949	0.9952	0.9962	0.9947	0.9951
J	0.0349	0.0430	0.0433	0.0614	0.2696
$L_{nom}(\%)$	-	23.2	24.1	75.9	672
$L_{opt}(\%)$	-	6.7	9.6	75.4	627

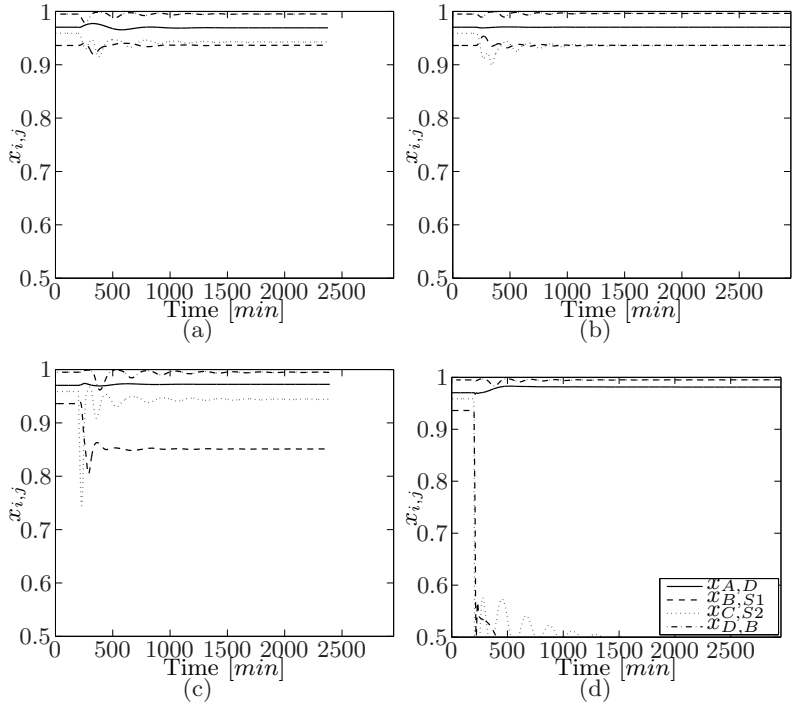

Figure 7.5: Kaibel column with 3 temperature loops closed: Disturbance responses (a) $F + 10\%$, (b) $z_{B,F} + 20\%$, (c) $R_V + 10\%$ and (d) $R_V + 50\%$

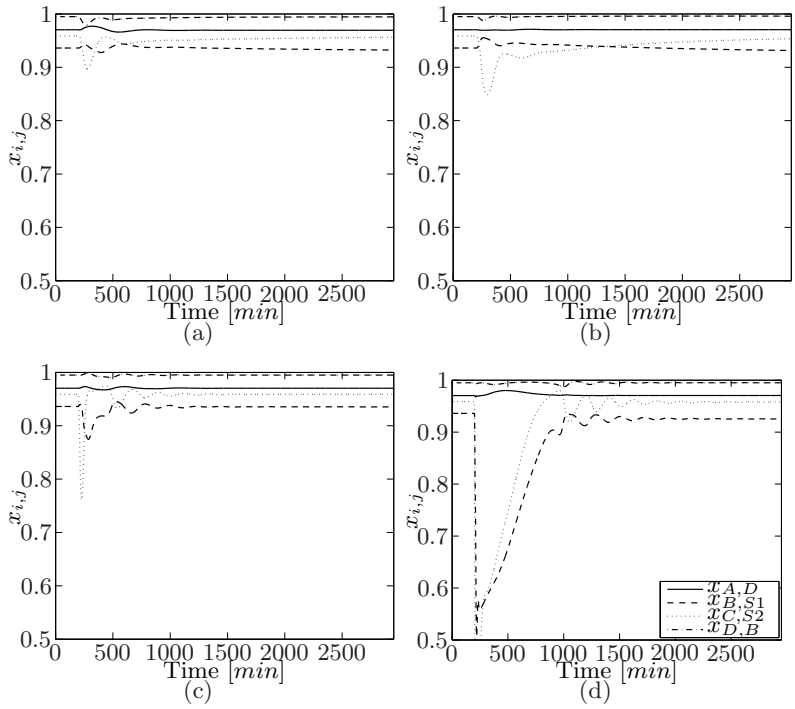

Figure 7.6: Kaibel column with four temperature loops closed: Disturbance responses (a) $F + 10\%$, (b) $z_{B,F} + 20\%$, (c) $R_V + 10\%$ and (d) $R_V + 50\%$

same disturbances as above. The dynamic responses for the configuration can be seen in Figure 7.6. Allthough the response to the changes in vapor split in Figures 7.6 (c) and 7.6 (d) show some dynamic variation, the extra temperature loop manages to reduce the loss in purity consideralbly as compared to the configurations where R_L is not used for control. The resulting purities, inputs, objective function value and percentage loss are given in Table 7.7 for the four disturbances. The table shows that the control configuration give very good disturbance rejection, and for the smaller change in R_V, nearly zero loss. The performance of all three control configurations are summarized in Table 7.8. Here we see clearly the improvement achieved when using the liquid split for control. The results confirm the findings of Halvorsen et al. [3], that either R_L or R_V needs to be adjusted online. Even for large disturbances in vapor split, the configurations with four temperature loops closed has very low loss.

*=0 because R_L is used for closed-loop control, so disturbances in R_L have no effect

Table 7.7: Kaibel column with 4 temperature loops closed: Effect of disturbances

	Nominal	ΔF_{+10}	$\Delta z_{B,F,+20}$	$\Delta R_{V,+10}$	$\Delta R_{V,+50}$
F	1.0000	1.1000	1.0000	1.0000	1.0000
$z_{B,F}$	0.2500	0.2500	0.3000	0.2500	0.2500
V	3.0000	3.0000	3.0000	3.0000	3.0000
R_L	0.2572	0.2434	0.2371	0.2969	0.4549
R_V	0.3770	0.3770	0.3770	0.4147	0.5655
L	2.8492	2.8349	2.8528	2.8496	2.8532
$S1$	0.2494	0.2746	0.3032	0.2498	0.2532
$S2$	0.2497	0.2753	0.2500	0.2499	0.2510
D	0.2508	0.2751	0.2472	0.2504	0.2468
B	0.2501	0.2750	0.1996	0.2499	0.2491
$x_{A,D}$	0.9703	0.9694	0.9706	0.9703	0.9705
x_{B,S_1}	0.9361	0.9324	0.9315	0.9354	0.9254
x_{C,S_2}	0.9589	0.9562	0.9535	0.9590	0.9580
$x_{D,B}$	0.9949	0.9945	0.9958	0.9949	0.9950
J	0.0349	0.0406	0.0405	0.0351	0.0380
L_{nom} (%)	-	16	16	0.6	8.9
L_{opt} (%)	-	0.7	2.5	0.3	2.4

Table 7.8: Kaibel column: Summary of objective function after disturbances

	1 loop		3 loops		4 loops	
	J $\left[\frac{mol}{min}\right]$	L_{nom} [%]	J $\left[\frac{mol}{min}\right]$	L_{nom} [%]	J $\left[\frac{mol}{min}\right]$	L_{nom} [%]
Nominal	0.0349	-	0.0349	-	0.0349	-
$\Delta R_L = -50\%$	0.1626	366	0.1332	282	0.0349	0*
$\Delta R_L = -25\%$	0.0932	167	0.0769	120	0.0349	0*
$\Delta R_L = +25\%$	0.0657	88	0.0576	65	0.0349	0*
$\Delta R_L = +50\%$	0.1027	194	0.1113	219	0.0349	0*
$\Delta F = +10\%$	0.0955	174	0.0430	23	0.0406	16
$\Delta z_{B,F} = +20\%$	0.1181	238	0.0433	24	0.0405	16
$\Delta R_V = +10\%$	0.0718	106	0.0614	76	0.0351	0.6
$\Delta R_V = +50\%$	0.2876	724	0.2696	672	0.0380	8.9

7.4 Petlyuk Column

The Petlyuk column (7.7) modelled here is similar to the Kaibel column in that it has the same number of stages in each column section except for the prefractionator sections which have 8 stages above the feed (section 1) and 8 stages below the feed (section 2), as opposed to 12 in each for the Kaibel column. It has also one column section less than the Kaibel column since we here only have 3 product streams. We use 3 components, which are the same components as the three heaviest in the Kaibel model (these are modeled as ethanol, propanol and butanol, but mainly referred to as A, B and C). The feed is again equimolar, but we have halved the ratio of vapor boilup to feed flow (V/F) as compared to the Kaibel column to account for the easier separation. The nominal optimal operating point for the Petlyuk arrangement is found by optimization with the objective to minimize total impurity flow in the products.

Analogous to the investigations on the Kaibel column, we want to look at control configurations for the Petlyuk column with varying number of temperature loops. The control configurations can be seen in Figure 7.8.

1. One temperature loop: Reflux, L, is used for temperature control (Also used in the other cases) (Fig. 7.8a)

2. Two temperature loops: Adding a temperature loop for the side stream (Fig 7.8b)

3. Three temperature loops: Adding a temperature loop for the liquid split, R_L (Fig 7.8c)

Initially, we will look at the two configurations that do not include R_L as an input.

7.4.1 Effect of liquid split ratio

For the two configurations (Figure 7.8 a) and b)), we set the liquid split ratio away from the optimum value and observe how this affects the product purities. The changes in R_L are $\pm 25\%$ and $\pm 50\%$ of the optimal value.

Input values, resulting product purities, objective function value and percentage loss for the case with one temperature loop can be seen in Table 7.9, while the values for the column with two temperature loops closed are shown in Table 7.10. The calculated loss in the objective function does not differ markedly for the two configurations, allthough the loss for the negative perturbations in R_L for the one-loop configuration is about twice

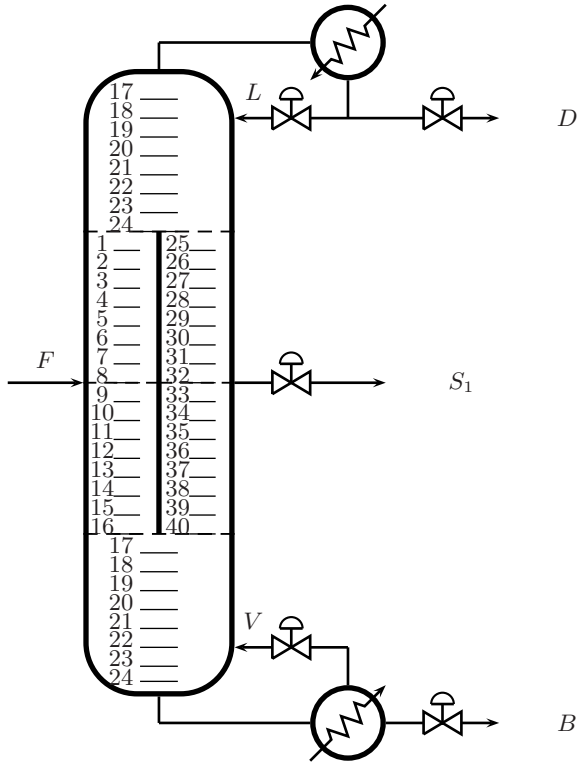

Figure 7.7: Petlyuk dividing-wall column. Stage numbering

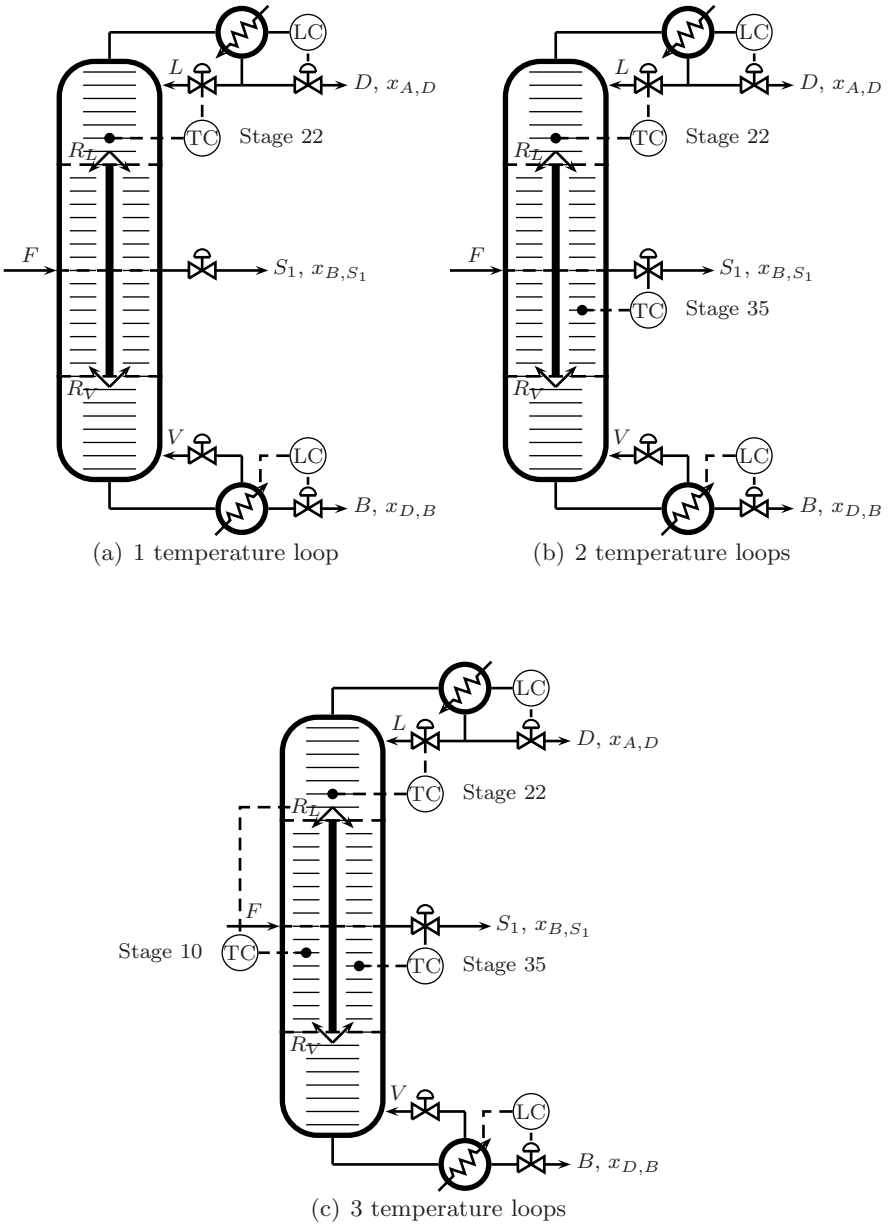

Figure 7.8: Petlyuk column control configurations (In all cases F, V and R_V are fixed)

Table 7.9: Petlyuk column with 1 temperature loop closed: Effect of changes in R_L

	$\Delta R_{L,-50}$	$\Delta R_{L,-25}$	Nominal	$\Delta R_{L,+25}$	$\Delta R_{L,+50}$
R_L	**0.1658**	**0.2487**	**0.3316**	**0.4145**	**0.4974**
F	1.0000	1.0000	1.0000	1.0000	1.0000
$z_{i,F}$	0.3333	0.3333	0.3333	0.3333	0.3333
V	1.5000	1.5000	1.5000	1.5000	1.5000
R_V	0.5346	0.5346	0.5346	0.5346	0.5346
L	1.2987	1.2744	1.2673	1.2695	1.2786
$S1$	0.3356	0.3356	0.3356	0.3356	0.3356
D	0.3013	0.3256	0.3327	0.3304	0.3214
B	0.3631	0.3388	0.3317	0.3339	0.3430
$x_{A,D}$	0.9881	0.9868	0.9862	0.9863	0.9866
x_{B,S_1}	0.7997	0.9144	0.9646	0.9442	0.8826
$x_{C,B}$	0.8310	0.9346	0.9849	0.9642	0.9043
J	0.1322	0.0552	0.0215	0.0352	0.0765
L_{nom} (%)	515	157	-	64	256

that of the two-loop column. For the positive perturbations, the one-loop configuration performs slightly better than the one with two temperature loops. Interestingly, this is the same as for the Kaibel column.

The temperature profiles of the Petlyuk column operating points for case 2 can be seen in Figure 7.9. Like for the Kaibel column we observe the shifting of the prefractionator temperature profile with varying R_L.

The composition profiles of the Petlyuk column operating points can be seen in Figure 7.10. The Petlyuk column arrangment does not require a sharp split between adjacent components in the prefractionator as the Kaibel column. However, for successful operation, the A/C split must be achieved in the prefractionator in the Petlyuk column. For an incorrectly implemented reflux split (R_L), we can see from Figure 7.10 c) and d) that some of component C is carried over the top of the prefractionator, causing the sidestream product to be less pure.

7.4.2 Disturbance rejection

As with the Kaibel column we apply disturbances to the two control configurations of the Petlyuk column. The disturbances introduced are the same as for the Kaibel column example above. That is, 10% increase in F, 20% increase in $z_{B,F}$, and 10% and 50% increase in R_V. The feed composition

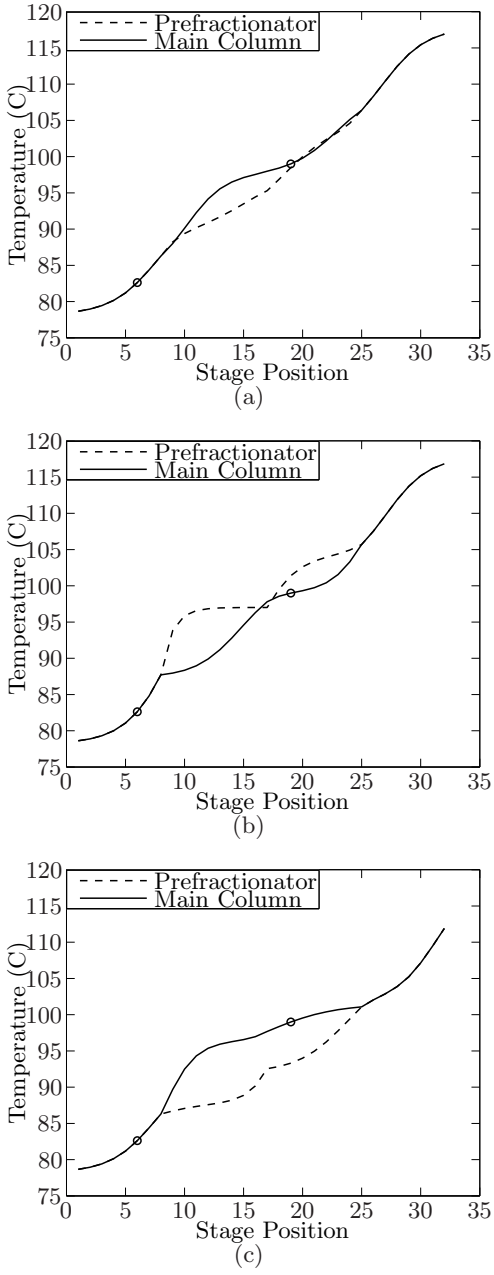

Figure 7.9: Petlyuk column with 2 temperature loops closed: Column temperature profiles. (a) Nominal profile, (b) $R_L = 0.50R_{L,opt}$, (c) $R_L = 1,50R_{L,opt}$. Controlled temperatures are circled.

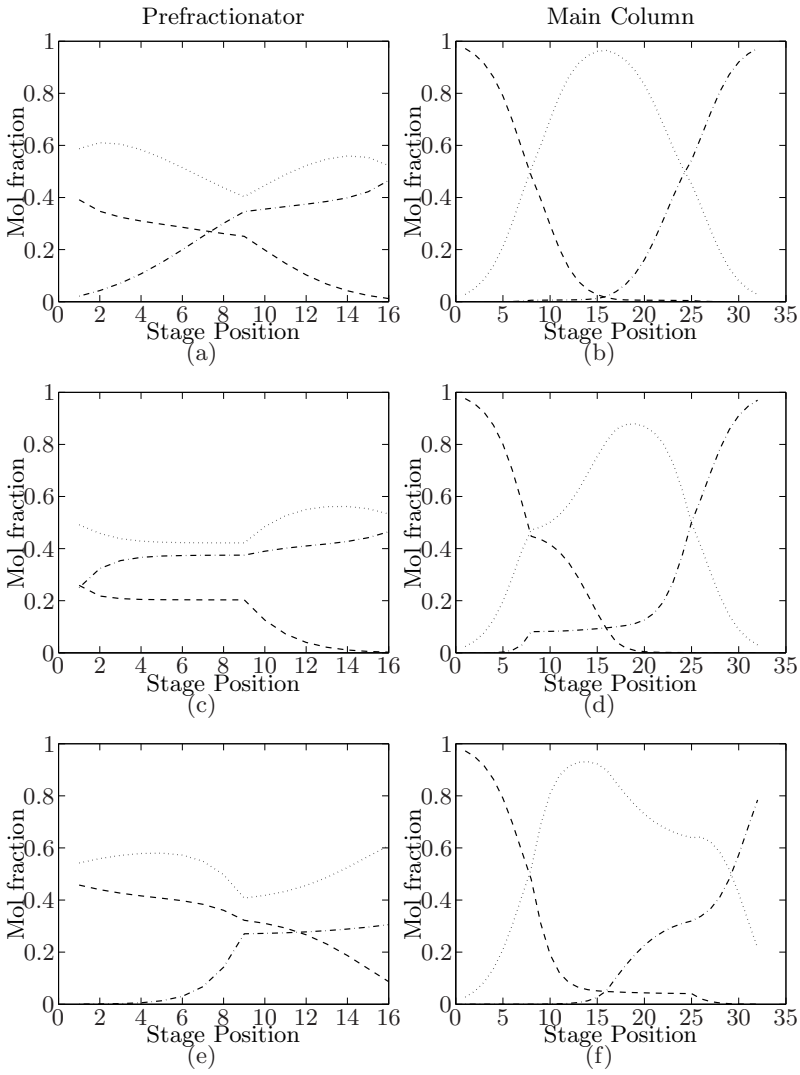

Figure 7.10: Petlyuk column with 2 temperature loops closed: Composition profiles of prefractionator and main column. (a) and (b) nominal operating point, (c) and (d) R_L is too low, (e) and (f) R_L is too high. ($- - -$ component A, $\cdots$ component B, $- \cdot -$ component C)

Table 7.10: Petlyuk column with 2 temperature loops closed: Effect of changes in R_L

	$\Delta R_{L,-50}$	$\Delta R_{L,-25}$	Nominal	$\Delta R_{L,+25}$	$\Delta R_{L,+50}$
R_L	**0.1658**	**0.2487**	**0.3316**	**0.4145**	**0.4974**
F	1.0000	1.0000	1.0000	1.0000	1.0000
$z_{i,F}$	0.3333	0.3333	0.3333	0.3333	0.3333
V	1.5000	1.5000	1.5000	1.5000	1.5000
R_V	0.5346	0.5346	0.5346	0.5346	0.5346
L	1.2997	1.2746	1.2673	1.2694	1.2777
$S1$	0.3997	0.3574	0.3356	0.3282	0.3135
D	0.3003	0.3254	0.3327	0.3306	0.3223
B	0.3000	0.3173	0.3317	0.3412	0.3642
$x_{A,D}$	0.9882	0.9869	0.9862	0.9863	0.9866
x_{B,S_1}	0.8128	0.9122	0.9646	0.9520	0.8986
$x_{C,B}$	0.9836	0.9903	0.9849	0.9520	0.8702
J	0.0833	0.0388	0.0215	0.0367	0.0834
L_{nom} (%)	287	80	-	71	288

increase in component B also implies a corresponding reduction in component C. Also here we include the reoptimized values for each disturbance for comparison. The optimal inputs can be seen in Table 7.11.

Tables 7.13 and 7.14 show the relevant inputs, resulting purities and objective function values after the disturbances for the two configurations. We observe that the two-loop configuration can handle the disturbances generally much better than the one-loop implementation, which is to be expected. For the large disturbance in R_V, however, both configurations are far off the optimum. The one-loop configuration have large impurities in both side stream and bottoms stream, while the two-loop configuration only suffers the impurity of the side stream (the distillate and bottoms get more pure).

The dynamic responses to the disturbances for the case with two temperature loops can be seen in Figure 7.11. The effect of the large change in R_V on the side stream composition is clearly visible.

Table 7.11: Petlyuk column: Optimal operating point for disturbances R_V fixed

	ΔF_{+10}	$\Delta z_{B,F,+20}$	$\Delta R_{V,+10}$	$\Delta R_{V,+50}$
F	1.1000	1.0000	1.0000	1.0000
$z_{B,F}$	0.3333	0.4000	0.3333	0.3333
V	1.5000	1.5000	1.5000	1.5000
R_L	0.3159	0.3096	0.3822	0.5888
R_V	0.5346	0.5346	0.5881	0.8020
L	1.2447	1.2675	1.2669	1.2661
S_1	0.3716	0.4041	0.3343	0.3314
D	0.3653	0.3325	0.3331	0.3339
B	0.3631	0.2634	0.3326	0.3346
$x_{A,D}$	0.9835	0.9828	0.9844	0.9531
x_{B,S_1}	0.9505	0.9635	0.9655	0.9351
$x_{C,B}$	0.9795	0.9813	0.9838	0.9769
$J_{opt,d}$	0.0318	0.0254	0.0221	0.0449

Table 7.12: Petlyuk column: Optimal operating point for disturbances R_L and R_V fixed

	Nominal	ΔF_{+10}	$\Delta z_{B,F,+20}$	$\Delta R_{V,+10}$	$\Delta R_{V,+50}$
F	1.0000	1.1000	1.0000	1.0000	1.0000
$z_{B,F}$	0.3333	0.3333	0.4000	0.3333	0.3333
V	1.5000	1.5000	1.5000	1.5000	1.5000
R_L	0.3316	0.3316	0.3316	0.3316	0.3316
R_V	0.5346	0.5346	0.5346	0.5881	0.8020
L	1.2673	1.2460	1.2687	1.2658	1.3112
S_1	0.3356	0.3704	0.4041	0.3395	0.4209
D	0.3327	0.3640	0.3313	0.3342	0.2888
B	0.3317	0.3656	0.2646	0.3263	0.2903
$x_{A,D}$	0.9862	0.9852	0.9851	0.9783	0.9307
x_{B,S_1}	0.9646	0.9510	0.9624	0.9511	0.7376
$x_{C,B}$	0.9849	0.9752	0.9767	0.9902	0.9901
J	0.0215	0.0326	0.0263	0.0270	0.1333

Table 7.13: Petlyuk column with 1 temperature loop closed: Effect of disturbances

	Nominal	ΔF_{+10}	$\Delta z_{B,F,+20}$	$\Delta R_{V,+10}$	$\Delta R_{V,+50}$
F	1.0000	1.1000	1.0000	1.0000	1.0000
$z_{B,F}$	0.3333	0.3333	0.4000	0.3333	0.3333
V	1.5000	1.5000	1.5000	1.5000	1.5000
R_L	0.3316	0.3316	0.3316	0.3316	0.3316
R_V	0.5346	0.5346	0.5346	0.5881	0.8020
L	1.2673	1.2454	1.2688	1.2763	1.4006
S_1	0.3356	0.3356	0.3356	0.3356	0.3356
D	0.3327	0.3646	0.3312	0.3237	0.1994
B	0.3317	0.3997	0.3332	0.3407	0.4650
$x_{A,D}$	0.9862	0.9849	0.9863	0.9867	0.9911
x_{B,S_1}	0.9646	0.9644	0.9731	0.9354	0.5308
$x_{C,B}$	0.9849	0.9062	0.7933	0.9557	0.6699
J	0.0215	0.0550	0.0824	0.0411	0.3127
L_{nom} (%)	-	156	283	91.2	1350
L_{opt} (%)	-	73.0	224	86.0	596

Table 7.14: Petlyuk column with 2 temperature loops closed: Effect of disturbances

	Nominal	ΔF_{+10}	$\Delta z_{B,F,+20}$	$\Delta R_{V,+10}$	$\Delta R_{V,+50}$
F	1.0000	1.1000	1.0000	1.0000	1.0000
$z_{B,F}$	0.3333	0.3333	0.4000	0.3333	0.3333
V	1.5000	1.5000	1.5000	1.5000	1.5000
R_L	0.3316	0.3316	0.3316	0.3316	0.3316
R_V	0.5346	0.5346	0.5346	0.5881	0.8020
L	1.2673	1.2357	1.2696	1.2696	1.4438
S_1	0.3356	0.3665	0.4050	0.4050	0.6043
D	0.3327	0.3643	0.3304	0.3304	0.1562
B	0.3317	0.3693	0.2646	0.2646	0.2395
$x_{A,D}$	0.9862	0.9849	0.9863	0.9867	0.9926
x_{B,S_1}	0.9646	0.9551	0.9614	0.9312	0.5495
$x_{C,B}$	0.9849	0.9697	0.9768	0.9908	0.9996
J	0.0215	0.0331	0.0263	0.0314	0.2735
L_{nom} (%)	-	54.0	22.3	46.0	1170
L_{opt} (%)	-	4.1	3.5	42.1	509

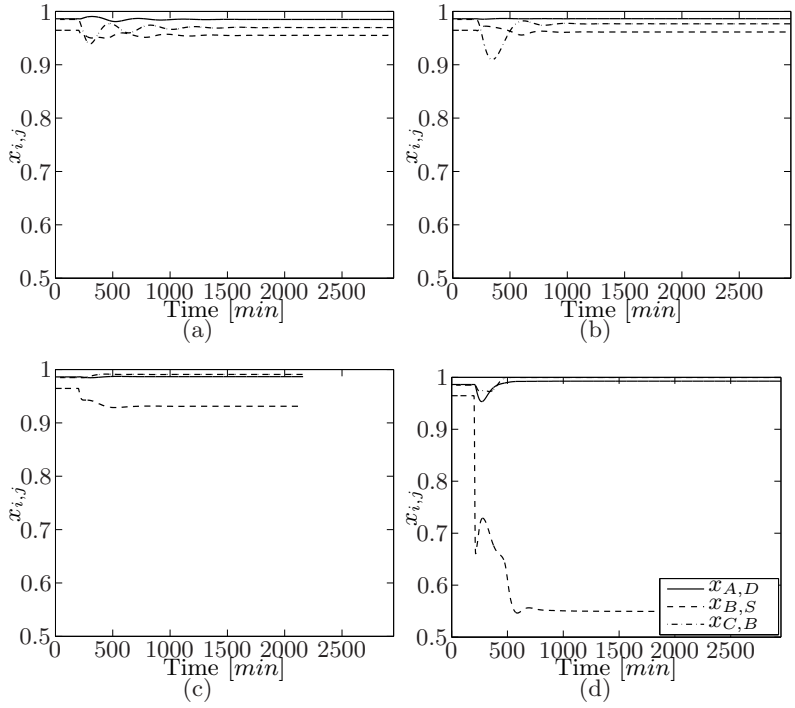

Figure 7.11: Petlyuk column with 2 temperature loops closed: Disturbance responses (a) $F + 10\%$, (b) $z_{B,F} + 20\%$, (c) $R_L + 10\%$ and (d) $R_V + 50\%$

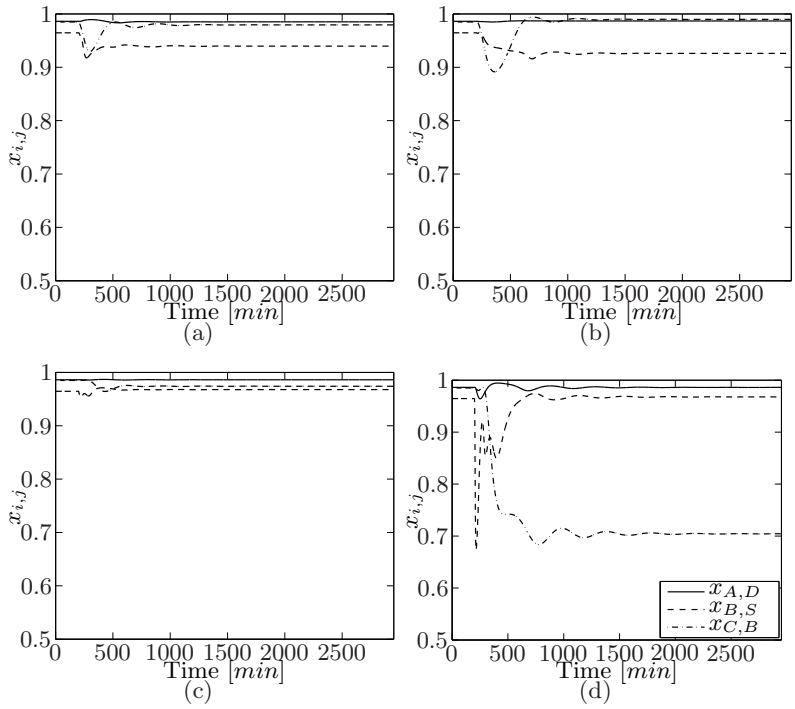

Figure 7.12: Petlyuk column with three temperature loops closed: Disturbance responses (a) F+10%, (b) $z_{B,F}$+20%, (c) R_V+10% and (d) R_V+50%

7.4.3 Petlyuk column with three temperature loops

Similarly to the Kaibel column we also include an extra temperature loop using the liquid split for the Petlyuk dividing-wall columnn. Figure 7.8 (c) shows the temperature loop that has been added. Again, we choose to control a temperature in the prefractionator section of the column.

The three-loop configuration is also tested with the selected disturbances defined above, and response plots for the column are shown in Figure 7.12. We notice that the extra loop cannot readily reject the large change in the vapor split, contrary to what we saw for the Kaibel column. Though a straight comparison is not justified since the increase in R_V in absolute terms is larger in this case. The inputs, resulting product purities, objective function values and loss for the disturbance simulations can be seen in Table 7.15. We can note that the smaller increase in R_V is handled well by the control system. This suggests that up to a certain point, we may adjust the liquid split to compensate for an incorrectly set vapor split. However,

Table 7.15: Petlyuk column with 3 temperature loops closed: Effect of disturbances

	Nominal	ΔF_{+10}	$\Delta z_{B,F,+20}$	$\Delta R_{V,+10}$	$\Delta R_{V,+50}$
F	1.0000	1.1000	1.0000	1.0000	1.0000
$z_{B,F}$	0.3333	0.3333	0.4000	0.3333	0.3333
V	1.5000	1.5000	1.5000	1.5000	1.5000
R_L	0.3316	0.2844	0.2479	0.4081	0.7141
R_V	0.5346	0.5346	0.5346	0.5881	0.8020
L	1.2673	1.2372	1.2782	1.2670	1.2647
S_1	0.3356	0.3766	0.4246	0.3307	0.1966
D	0.3327	0.3628	0.3218	0.3330	0.3353
B	0.3317	0.3606	0.2536	0.3363	0.4681
$x_{A,D}$	0.9862	0.9851	0.9868	0.9862	0.9861
x_{B,S_1}	0.9646	0.9397	0.9260	0.9677	0.9678
$x_{C,B}$	0.9849	0.9795	0.9898	0.9741	0.7044
J	0.0215	0.0355	0.0382	0.0240	0.1494
L_{nom} (%)	-	65.1	77.7	11.6	595
L_{opt} (%)	-	11.6	50.3	8.6	233

in this case the problem has more to do with the side stream and bottoms rates. They are far off the optimum, and it would be better to keep them constant, though this is not easily achieved in practice.

The performance of all three control configurations is summarized in Table 7.16. The benefit of the extra (R_L) loop is not so evident here as it was for the Kaibel column, except for the disturbances in R_V. When the feed composition is changed, the two-loop configuration is considerably better than the three-loop configuration. The locations of the temperature measurements could have a large effect here, and it is likely that other locations can be found that will improve the performance of the three-loop configuration over the other two.

Table 7.16: Petlyuk column: Summary of objective function values after disturbances

	1 loop		2 loops		3 loops	
	J $\left[\frac{mol}{min}\right]$	L_{nom} [%]	J $\left[\frac{mol}{min}\right]$	L_{nom} [%]	J $\left[\frac{mol}{min}\right]$	L_{nom} [%]
Nominal	0.0215	-	0.0215	-	0.0215	-
$\Delta R_L = -50\%$	0.1322	515	0.0833	287	0.0215	0
$\Delta R_L = -25\%$	0.0552	157	0.0388	81	0.0215	0
$\Delta R_L = +25\%$	0.0352	64	0.0367	71	0.0215	0
$\Delta R_L = +50\%$	0.0765	256	0.0834	288	0.0215	0
$\Delta F = +10\%$	0.0550	156	0.0331	54	0.0355	65
$\Delta z_{B,F} = +20\%$	0.0824	283	0.0263	22	0.0382	78
$\Delta R_V = +10\%$	0.0411	91	0.0314	46	0.0240	12
$\Delta R_V = +50\%$	0.3127	1350	0.2735	1170	0.1494	595

7.5 High-purity dividing-wall columns

In the examples presented above, the product purities have not been particularly high because of the low number of stages modelled. It would therfore be interesting to see if a high-purity column would behave differently and especially whether high-purity columns are more sensitive to the liquid split. In the following we present a Kaibel column and a Petlyuk column with high nominal purities of the products.

7.5.1 High-purity Kaibel column

This column has twice as many stages as the previous model of the Kaibel column. That is, 24 stages in each of the two prefractionator sections and 16 in each of the other column sections. The resulting product purities are all above 99.7% at the nominal optimum.

Effect of liquid split

Following the analysis from the previous section, we first look at the effects of setting the liquid split ratio away from the optimal value for a Kaibel column with 1 and 3 temperature loops closed respectively. The resulting product purities and objective function values can be seen in Table 7.17 for the case with only one temperature loop closed. The results for the column with three temperature loops can are shown in Table 7.18. We can immediately see that this column is very sensitive to an incorrectly set liquid

Table 7.17: High-purity Kaibel column with 1 temperature loop: Effect of changes in R_L

	$\Delta R_{L,-50}$	$\Delta R_{L,-25}$	Nominal	$\Delta R_{L,+25}$	$\Delta R_{L,+50}$
R_L	0.2144	0.3216	0.4288	0.5360	0.6433
F	1.0000	1.0000	1.0000	1.0000	1.0000
$z_{i,F}$	0.2500	0.2500	0.2500	0.2500	0.2500
V	3.0000	3.0000	3.0000	3.0000	3.0000
R_V	0.5407	0.5407	0.5407	0.5407	0.5407
L	2.8520	2.8508	2.8498	2.8497	2.8623
$S1$	0.2496	0.2496	0.2496	0.2496	0.2496
$S2$	0.2498	0.2498	0.2498	0.2498	0.2498
D	0.2480	0.2492	0.2502	0.2503	0.2377
B	0.2526	0.2514	0.2504	0.2502	0.2629
$x_{A,D}$	0.9991	0.9988	0.9984	0.9984	0.9985
x_{B,S_1}	0.5657	0.7380	0.9977	0.8164	0.6218
x_{C,S_2}	0.5388	0.7378	0.9976	0.8164	0.5989
$x_{D,B}$	0.9387	0.9952	0.9984	0.9985	0.9499
J	0.2393	0.1324	0.0020	0.0925	0.2081
L_{nom} (%)	$\sim$ 12000	$\sim$ 6500	-	$\sim$ 4500	$\sim$ 10300

split than the column with lower purities. This agrees with the findings of Halvorsen and Skogestad [4] The second thing to note, is that the effect of the liquid split change is almost the same for the two configurations.

Disturbance rejection

Next, we look at changes in the disturbance variables that we have been using throughout this chapter. The optimal values for the disturbances can be seen in Table 7.19. Table 7.21 shows the resulting purities, input values and objective function values after disturbances have been introduced to the configuration where only the reflux is used for temperature control. Table 7.22 shows the results for the high-purity Kaibel column with three temperature loops closed. Here we see some improvement in going from one to three temperature loops for the feed flow and feed composition changes, but the disturbance in vapor split has nearly the same effect on both configurations. Again, we note that the high-purity column is much more sensitive to these disturbances than the column with low number of stages.

Finally, we add the fourth temperature loop using the liquid split for control. The resulting values after disturbances are given in Table 7.23.

Table 7.18: High-purity Kaibel column with 3 temperature loops: Effect of changes in R_L

	$\Delta R_{L,-50}$	$\Delta R_{L,-25}$	Nominal	$\Delta R_{L,+25}$	$\Delta R_{L,+50}$
R_L	**0.2144**	**0.3216**	**0.4288**	**0.5360**	**0.6433**
F	1.0000	1.0000	1.0000	1.0000	1.0000
$z_{i,F}$	0.2500	0.2500	0.2500	0.2500	0.2500
V	3.0000	3.0000	3.0000	3.0000	3.0000
R_V	0.5407	0.5407	0.5407	0.5407	0.5407
L	2.8520	2.8508	2.8498	2.8497	2.8625
$S1$	0.2477	0.2564	0.2496	0.2249	0.2393
$S2$	0.2674	0.2440	0.2498	0.2747	0.2739
D	0.2480	0.2492	0.2502	0.2503	0.2375
B	0.2369	0.2504	0.2504	0.2501	0.2493
$x_{A,D}$	0.9991	0.9988	0.9984	0.9984	0.9985
x_{B,S_1}	0.5657	0.7381	0.9977	0.8850	0.6178
x_{C,S_2}	0.5630	0.7522	0.9976	0.8163	0.6037
$x_{D,B}$	0.9987	0.9984	0.9984	0.9995	0.9998
J	0.2250	0.1283	0.0020	0.0768	0.2004
L_{nom} (%)	$\sim$ 11300	$\sim$ 6400	-	$\sim$ 3800	$\sim$ 10100

Table 7.19: High-purity Kaibel column: Optimal operating points for disturbances

	ΔF_{+10}	$\Delta z_{B,F,+20}$	$\Delta R_{V,+10}$	$\Delta R_{V,+50}$
F	1.1000	1.0000	1.0000	1.0000
$z_{i,F}$	0.2500	0.3000	0.2500	0.2500
V	3.0000	3.0000	3.0000	3.0000
R_L	0.4170	0.4113	0.4857	0.7132
R_V	0.5407	0.5407	0.5948	0.8111
L	2.8348	2.8500	2.8499	2.8510
S_1	0.2745	0.2998	0.2496	0.2504
S_2	0.2745	0.2499	0.2499	0.2508
D	0.2652	0.2500	0.2501	0.2490
B	0.1857	0.2003	0.2505	0.2497
$x_{A,D}$	0.9981	0.9983	0.9984	0.9949
x_{B,S_1}	0.9975	0.9972	0.9975	0.9904
x_{C,S_2}	0.9977	0.9976	0.9975	0.9939
$x_{D,B}$	0.9973	0.9986	0.9981	0.9979
$J_{opt,d}$	0.0026	0.0021	0.0021	0.0057

Table 7.20: High-purity Kaibel column: Optimal operating points for disturbances fixed R_L and R_V

	Nominal	ΔF_{+10}	$\Delta z_{B,F,+20}$
F	1.0000	1.1000	1.0000
$z_{i,F}$	0.2500	0.2500	0.3000
V	3.0000	3.0000	3.0000
R_L	0.4288	0.4288	0.4288
R_V	0.5407	0.5407	0.5407
L	2.8498	2.8346	2.8494
S_1	0.2496	0.2696	0.2926
S_2	0.2495	0.2799	0.2567
D	0.2502	0.2654	0.2506
B	0.2508	0.1851	0.2001
$x_{A,D}$	0.9984	0.9977	0.9968
x_{B,S_1}	0.9977	0.9974	0.9973
x_{C,S_2}	0.9976	0.9803	0.9712
$x_{D,B}$	0.9969	0.9996	0.9996
J	0.0023	0.0069	0.0091

Table 7.21: High-purity Kaibel column with 1 temperature loop closed: Effect of disturbances

	Nominal	ΔF_{+10}	$\Delta z_{B,F,+20}$	$\Delta R_{V,+10}$	$\Delta R_{V,+50}$
F	1.0000	1.1000	1.0000	1.0000	1.0000
$z_{B,F}$	0.2500	0.2500	0.3000	0.2500	0.2500
V	3.0000	3.0000	3.0000	3.0000	3.0000
R_L	0.4288	0.4288	0.4288	0.4288	0.4288
R_V	0.5407	0.5407	0.5407	0.5948	0.8111
L	2.8498	2.8347	2.8498	2.8506	2.9676
$S1$	0.2496	0.2496	0.2496	0.2496	0.2496
$S2$	0.2498	0.2498	0.2498	0.2498	0.2498
D	0.2502	0.2753	0.2502	0.2494	0.1323
B	0.2504	0.3253	0.2504	0.2512	0.3682
x_D	0.9984	0.9982	0.9984	0.9986	0.9993
x_{S_1}	0.9977	0.9991	0.9991	0.8339	0.5003
x_{S_2}	0.9976	0.8993	0.7989	0.8338	0.2643
x_B	0.9984	0.8454	0.7987	0.9965	0.6793
J	0.0020	0.0762	0.1013	0.0842	0.4268
L_{nom} (%)	-	$\sim$ 3700	$\sim$ 5000	$\sim$ 4100	$\sim$ 21200
L_{opt} (%)	-	$\sim$ 2800	$\sim$ 4700	$\sim$ 3900	$\sim$ 7400

Table 7.22: High-purity Kaibel column with 3 temperature loops closed: Effect of disturbances

	Nominal	ΔF_{+10}	$\Delta z_{B,F,+20}$	$\Delta R_{V,+10}$	$\Delta R_{V,+50}$
F	1.0000	1.1000	1.0000	1.0000	1.0000
$z_{B,F}$	0.2500	0.2500	0.3000	0.2500	0.2500
V	3.0000	3.0000	3.0000	3.0000	3.0000
R_L	0.4288	0.4288	0.4288	0.4288	0.4288
R_V	0.5407	0.5407	0.5407	0.5948	0.8111
L	2.8498	2.8347	2.8498	2.8506	2.9843
$S1$	0.2496	0.2636	0.2654	0.2600	0.2603
$S2$	0.2498	0.2856	0.2843	0.2403	0.3738
D	0.2502	0.2753	0.2502	0.2494	0.1157
B	0.2504	0.2755	0.2001	0.2504	0.2502
x_D	0.9984	0.9982	0.9984	0.9986	0.9995
x_{S_1}	0.9977	0.9989	0.9990	0.8339	0.3915
x_{S_2}	0.9976	0.9593	0.8782	0.8630	0.3945
x_B	0.9984	0.9982	0.9993	0.9985	0.9991
J	0.0020	0.0129	0.0354	0.0768	0.3850
L_{nom} (%)	-	~ 550	~ 1700	~ 3700	~ 19100
L_{opt} (%)	-	~ 400	~ 160	~ 3600	~ 6700

Table 7.23: High-purity Kaibel column with 4 temperature loops closed: Effect of disturbances

	Nominal	ΔF_{+10}	$\Delta z_{B,F,+20}$	$\Delta R_{V,+10}$	$\Delta R_{V,+50}$
F	1.0000	1.1000	1.0000	1.0000	1.0000
$z_{B,F}$	0.2500	0.2500	0.3000	0.2500	0.2500
V	3.0000	3.0000	3.0000	3.0000	3.0000
R_L	0.4288	0.4170	0.4113	0.4857	0.5354
R_V	0.5407	0.5407	0.5407	0.5948	0.8111
L	2.8498	2.8348	2.8500	2.8499	2.9401
$S1$	0.2496	0.2653	0.2661	0.2494	0.2605
$S2$	0.2498	0.2839	0.2838	0.2501	0.3293
D	0.2502	0.2752	0.2500	0.2501	0.1597
B	0.2504	0.2756	0.2001	0.2504	0.2505
x_D	0.9984	0.9982	0.9984	0.9984	0.9995
x_{S_1}	0.9977	0.9986	0.9984	0.9979	0.3534
x_{S_2}	0.9976	0.9652	0.8799	0.9958	0.4319
x_B	0.9984	0.9977	0.9992	0.9984	0.9990
J	0.0020	0.0114	0.0351	0.0023	0.3559
L_{nom} (%)	-	~ 470	~ 1700	~ 15	~ 17700
L_{opt} (%)	-	~ 340	~ 1600	~ 10	~ 6100

The improvement for the feed disturbances is minimal, but for the smaller change in vapor split the extra temperature loop manages to keep operation very close to the nominal point. A slight decrease in the second side stream (S_2) is the only result of the disturbance. The large perturbation in R_V however, is too much for the column to handle. *

Table 7.24 summarizes the results of all three control configurations.

7.5.2 High-purity Petlyuk column

The model of the high-purity Petlyuj column has also two times the number of stages as compared to the Petlyuk column in the previous examples.

The increased number of stages lead to changes in the dynamic behaviour of the column, and the temperature to be controlled by the sidestream valve had to be moved down in the bottom section as compared to the column with fewer stages, because of small process gain in the section directly below the sidestream. †

*Note to self, not part of thesis: change this!

†Note to self, not part of thesis: give stage nos or show figure

Table 7.24: High-purity Kaibel column: Summary of objective function values after disturbances

	1 loop		3 loops		4 loops	
	J $\left[\frac{mol}{min}\right]$	L_{nom} [%]	J $\left[\frac{mol}{min}\right]$	L_{nom} [%]	J $\left[\frac{mol}{min}\right]$	L_{nom} [%]
Nominal	0.0020	-	0.0020	-	0.0020	-
$\Delta R_L = -50\%$	0.2393	12000	0.2250	11300	0.0020	0
$\Delta R_L = -25\%$	0.1324	6500	0.1283	6400	0.0020	0
$\Delta R_L = +25\%$	0.0925	4500	0.0768	3800	0.0020	0
$\Delta R_L = +50\%$	0.2081	10300	0.2004	10100	0.0020	0
$\Delta F = +10\%$	0.0762	3700	0.0129	550	0.0114	470
$\Delta z_{B,F} = +20\%$	0.1013	5000	0.0354	1700	0.0351	1700
$\Delta R_V = +10\%$	0.0842	4100	0.0768	3700	0.0023	15
$\Delta R_V = +50\%$	0.4268	21200	0.3850	19100	0.3559	17700

Effect of liquid split

The liquid split ratio for the high-purity Petlyuk column is varied around the nominal optimal operating point for the control configurations with one and temperature loops respectively. The input values, resulting purities and objective function values for the case with only one temperature loop can be seen in Table 7.25. Table 7.26 show the values for the case with two temperature loops closed. As for the high-purity Kaibel column, the relative increase in the objective function is very large compared to the column with fewer stages when R_L is set away from its optimal value. We note that the configuration with two loops manages to keep the purities at both column ends, while the configuration with only the "reflux loop" gets large impurities in both side and bottoms streams.

Disturbance rejection

Like with the high-purity Kaibel column, we subject the different control configurations of the high-purity Petlyuk column to the selcted disturbances. The optimal inputs for the disturbances can be seen in Table 7.27.

First for the configuration with one temperature loop (Table 7.29) and the case with two temperature loops (Table 7.30). Finally, we add the third temperature loop, making use of the liquid split (R_L) for feedback control (Table 7.31). For the feed disturbances there is a great improvement in going from one to two temperature loops, where the losses are relatively small. However, for the change in vapor split, we see that we need the

Table 7.25: High-purity Petlyuk column with 1 temperature loop closed: Effect of changes in R_L

	$\Delta R_{L,-50}$	$\Delta R_{L,-25}$	Nominal	$\Delta R_{L,+25}$	$\Delta R_{L,+50}$
R_L	**0.1718**	**0.2577**	**0.3436**	**0.4295**	**0.5154**
F	1.0000	1.0000	1.0000	1.0000	1.0000
$z_{i,F}$	0.3333	0.3333	0.3333	0.3333	0.3333
V	1.5000	1.5000	1.5000	1.5000	1.5000
R_V	0.5515	0.5515	0.5515	0.5515	0.5515
L	1.3109	1.2767	1.2667	1.2676	1.2795
$S1$	0.3335	0.3335	0.3335	0.3335	0.3335
D	0.2891	0.3233	0.3333	0.3324	0.3205
B	0.3774	0.3432	0.3332	0.3340	0.3460
$x_{A,D}$	0.9998	0.9998	0.9998	0.9998	0.9998
x_{B,S_1}	0.7729	0.9211	0.9988	0.9890	0.8971
$x_{C,B}$	0.8000	0.9242	0.9996	0.9899	0.9016
J	0.1513	0.0524	0.0006	0.0071	0.0684
L_{nom} (%)	$\sim$ 24000	$\sim$ 8300	-	$\sim$ 1000	$\sim$ 11000

Table 7.26: High-purity Petlyuk column with 2 temperature loops closed: Effect of changes in R_L

	$\Delta R_{L,-50}$	$\Delta R_{L,-25}$	Nominal	$\Delta R_{L,+25}$	$\Delta R_{L,+50}$
R_L	**0.1718**	**0.2577**	**0.3436**	**0.4295**	**0.5154**
F	1.0000	1.0000	1.0000	1.0000	1.0000
$z_{i,F}$	0.3333	0.3333	0.3333	0.3333	0.3333
V	1.5000	1.5000	1.5000	1.5000	1.5000
R_V	0.5515	0.5515	0.5515	0.5515	0.5515
L	1.3109	1.2768	1.2667	1.2676	1.2815
$S1$	0.4173	0.3608	0.3335	0.3593	0.4278
D	0.2891	0.3232	0.3333	0.3324	0.3185
B	0.2936	0.3159	0.3332	0.3084	0.2537
$x_{A,D}$	0.9998	0.9998	0.9998	0.9998	0.9998
x_{B,S_1}	0.7984	0.9233	0.9988	0.9273	0.7790
$x_{C,B}$	0.9997	0.9996	0.9996	0.9997	0.9998
J	0.0843	0.0279	0.0006	0.0263	0.0947
L_{nom} (%)	$\sim$ 13500	$\sim$ 4400	-	$\sim$ 4100	$\sim$ 15000

Table 7.27: High-purity Petlyuk column: Optimal operating points for disturbances

	ΔF_{+10}	$\Delta z_{B,F,+20}$	$\Delta R_{V,+10}$	$\Delta R_{V,+50}$
F	1.1000	1.0000	1.0000	1.0000
$z_{B,F}$	0.3333	0.4000	0.3333	0.3333
V	1.5000	1.5000	1.5000	1.5000
R_L	0.3201	0.3048	0.3839	0.5955
R_V	0.5346	0.5346	0.5881	0.8020
L	1.2435	1.2668	1.2667	1.2680
S_1	0.3675	0.4010	0.3335	0.3354
D	0.3665	0.3332	0.3333	0.3320
B	0.3660	0.2658	0.3332	0.3326
$x_{A,D}$	0.9997	0.9998	0.9997	0.9952
x_{B,S_1}	0.9968	0.9971	0.9988	0.9875
$x_{C,B}$	0.9994	0.9997	0.9996	0.9984
$J_{opt,d}$	0.0015	0.0013	0.0006	0.0063

third temperature loop to compensate by adjusting the liquid split. This is in agreement with the results from the other columns investigated above. Also here, we see that the large disturbance in R_V cannot readily be rejected by any control configuration.

Table 7.32 summarizes the objective function values of the previous tables for the high-purity Petlyuk column.

7.6 Conclusions

In this chapter, we have studied the practical implementation of stabilizing control for dividing-wall distillation columns. The examples include the 4-product Kaibel column and the more well-known 3-product Petlyuk column. In the study, we assume that the objective is to maximize the purity of all product streams, and we show that setting the correct liquid split ratio is essential in achieving the potential purities. Control configurations with varying number of temperature loops have been tested and compared. We show that the liquid split can be used to control a temperature in the prefractionator section and thereby reduce the sensitivity to disturbances. Adjusting the liquid split is particularly important in reducing the column's sensitivity to the vapor split ratio. We also show that for high-purity columns the need to adjust the liquid split online is even greater.

Table 7.28: High-purity Petlyuk column: Optimal operating points for disturbances fixed R_L and R_V

	Nominal	ΔF_{+10}	$\Delta z_{B,F,+20}$	$\Delta R_{V,+10}$	$\Delta R_{V,+50}$
F	1.0000	1.1000	1.0000	1.0000	1.0000
$z_{B,F}$	0.3333	0.3333	0.4000	0.3333	0.3333
V	1.5000	1.5000	1.5000	1.5000	1.5000
R_L	0.3316	0.3316	0.3316	0.3316	0.3316
R_V	0.5346	0.5346	0.5346	0.5881	0.8020
L	1.2667	1.2436	1.2669	1.2669	1.3194
S_1	0.3335	0.3678	0.4014	0.3377	0.4306
D	0.3333	0.3664	0.3331	0.3331	0.2806
B	0.3332	0.3658	0.2654	0.3292	0.2887
$x_{A,D}$	0.9998	0.9997	0.9998	0.9997	0.9919
x_{B,S_1}	0.9988	0.9960	0.9961	0.9862	0.7687
$x_{C,B}$	0.9996	0.9993	0.9997	0.9994	0.9998
J	0.0006	0.0018	0.0017	0.0050	0.1019

Table 7.29: High-purity Petlyuk column with 1 temperature loop closed: Effect of disturbances

	Nominal	ΔF_{+10}	$\Delta z_{B,F,+20}$	$\Delta R_{V,+10}$	$\Delta R_{V,+50}$
F	1.0000	1.1000	1.0000	1.0000	1.0000
$z_{B,F}$	0.3333	0.3333	0.4000	0.3333	0.3333
V	1.5000	1.5000	1.5000	1.5000	1.5000
R_L	0.3436	0.3436	0.3436	0.3436	0.3436
R_V	0.5515	0.5515	0.5515	0.6067	0.8273
L	1.2667	1.2435	1.2668	1.2868	1.3882
$S1$	0.3335	0.3335	0.3335	0.3335	0.3335
D	0.3333	0.3665	0.3332	0.3132	0.2118
B	0.3332	0.3999	0.3332	0.3532	0.4546
x_D	0.9998	0.9997	0.9998	0.9998	0.9999
x_{S_1}	0.9988	0.9985	0.9991	0.9303	0.5648
x_B	0.9996	0.9162	0.7999	0.9350	0.6812
J	0.0006	0.0341	0.0671	0.0463	0.2901
L_{nom} (%)	-	$\sim$ 5600	$\sim$ 11000	$\sim$ 7600	$\sim$ 48000
L_{opt} (%)		$\sim$ 2200	$\sim$ 5100	$\sim$ 7600	$\sim$ 4500

Table 7.30: High-purity Petlyuk column with 2 temperature loops closed: Effect of disturbances

	Nominal	ΔF_{+10}	$\Delta z_{B,F,+20}$	$\Delta R_{V,+10}$	$\Delta R_{V,+50}$
F	1.0000	1.1000	1.0000	1.0000	1.0000
$z_{B,F}$	0.3333	0.3333	0.4000	0.3333	0.3333
V	1.5000	1.5000	1.5000	1.5000	1.5000
R_L	0.3436	0.3436	0.3436	0.3436	0.3436
R_V	0.5515	0.5515	0.5515	0.6067	0.8273
L	1.2667	1.2435	1.2668	1.2868	1.4293
$S1$	0.3335	0.3682	0.4014	0.3567	0.5370
D	0.3333	0.3665	0.3332	0.3132	0.1707
B	0.3332	0.3653	0.2654	0.3301	0.2923
x_D	0.9998	0.9997	0.9998	0.9998	0.9999
x_{S_1}	0.9988	0.9951	0.9961	0.9341	0.6206
x_B	0.9996	0.9995	0.9997	0.9996	0.9997
J	0.0006	0.0021	0.0017	0.0237	0.2038
L_{nom} (%)	-	~ 250	~ 180	~ 3900	~ 34000
L_{opt} (%)	-	~ 40	~ 30	~ 3900	~ 3100

Table 7.31: High-purity Petlyuk column with 3 temperature loops closed: Effect of disturbances

	Nominal	ΔF_{+10}	$\Delta z_{B,F,+20}$	$\Delta R_{V,+10}$	$\Delta R_{V,+50}$
F	1.0000	1.1000	1.0000	1.0000	1.0000
$z_{B,F}$	0.3333	0.3333	0.4000	0.3333	0.3333
V	1.5000	1.5000	1.5000	1.5000	1.5000
R_L	0.3436	0.3331	0.3223	0.3979	0.6403
R_V	0.5515	0.5515	0.5515	0.6067	0.8273
L	1.2667	1.2435	1.2669	1.2669	1.3192
$S1$	0.3335	0.3677	0.4009	0.3337	0.4412
D	0.3333	0.3665	0.3331	0.3331	0.2808
B	0.3332	0.3658	0.2659	0.3332	0.2780
x_D	0.9998	0.9997	0.9998	0.9998	0.9998
x_{S_1}	0.9988	0.9965	0.9973	0.9983	0.7552
x_B	0.9996	0.9995	0.9997	0.9996	0.9997
J	0.0006	0.0016	0.0013	0.0008	0.1081
L_{nom} (%)	-	~ 170	~ 120	~ 30	~ 18000
L_{opt} (%)	-	~ 7	~ 0	~ 30	~ 1600

Table 7.32: High-purity Petlyuk column: Summary of objective function values after disturbances

	1 loop		2 loops		3 loops	
	J $\left[\frac{mol}{min}\right]$	L_{nom} $[\%]$	J $\left[\frac{mol}{min}\right]$	L_{nom} $[\%]$	J $\left[\frac{mol}{min}\right]$	L_{nom} $[\%]$
Nominal	0.0006	-	0.0006	-	0.0006	-
$\Delta R_L = -50\%$	0.1513	24000	0.0843	13500	0.0006	0
$\Delta R_L = -25\%$	0.0524	8300	0.0279	4400	0.0006	0
$\Delta R_L = +25\%$	0.0071	1000	0.0263	4100	0.0006	0
$\Delta R_L = +50\%$	0.0684	11000	0.0947	15000	0.0006	0
$\Delta F = +10\%$	0.0341	5600	0.0021	250	0.0016	170
$\Delta z_{B,F} = +20\%$	0.0671	11000	0.0017	180	0.0012	120
$\Delta R_V = +10\%$	0.0463	7600	0.0237	3900	0.0008	30
$\Delta R_V = +50\%$	0.2901	48000	0.2038	34000	0.1081	18000

Chapter 8

Optimal Operation -Bottom-up design

8.1 Regulatory control layer

The purpose of a regulatory control layer is to stabilize the operation of the plant, here the Kaibel distillation column. Even if the column is not inherently unstable in the mathematical sense, any distillation column will -in addition to drift in the liquid levels, be subject to a "drift" in its composition profile away from the operating point [5,].

The regulatory control layer for a distillation column usually includes pressure control and control of liquid levels in the reboiler and condenser. In this work the choice of level control configuration is not investigated, and the L/V-configuration is used in all examples. Pressure control is also omitted since the analytical model assumes uniform pressure.

The task here is to find a set of secondary variables y_2 to control using manipulated inputs u_2, to avoid drift. The setpoints for the secondary variables y_{2s} may be used as inputs for the upper layer's primary controlled variables. *

Maintaining splits in the Kaibel column

†

In order to avoid "drift" in the column with undesirable breakthrough of impurities in the product we need to stabilize the column profile. In this

*Note to self, not part of thesis: refer to chapter 2 where more on basis for regulatory control

†Note to self, not part of thesis: more cutouts here

sense, we can view the Kaibel column as essentially 4 columns within the one. Firstly, in the prefractionator we need to maintain the split between components B and C. In the main column, there are three "internal profiles" that must be maintained. We need to keep the split between A and B in the top (sections 3 & 4). In the middle section (section 7) there is a B/C-split, and the C/D-split in the bottom (sections 5 & 6) must be maintained. This requires closing 4 regulatory control loops, and we need to find suitable measurements and pair them with the available inputs. These loops need to be relatively fast, and since composition measurements are usually slow (large effective time delay) and with variable reliability, we propose to use temperatures as the controlled variables.

Temperature loop

*

8.2 Selection of secondary controlled variables

8.3 Criteria for measurement selection

As mentioned, the regulatory control layer should stabilize the plant operation, and the focus is now on dynamic performance as opposed to the steady-state economic criteria used in selecting the primary controlled variables. If possible, we would like the regulatory control to be independent of the layer above. That is, we want the control structure (of the regulatory layer) to be independent of the operational mode (Section 5.2) and the operating point of the column.

We will here apply different criteria for the selection of temperature locations and compare them. We also apply the minimum singular value method [4] for selecting the controlled variables to some of the operational modes outlined in Section 5.2 . The procedure for the method is described in Chapter 2.

Temperature Locations

The analysis shown here assumes a temperature measurement at every stage in the column. This is unlikely to be found in "real-life" implementations, but we may use the analysis as a design procedure to decide on where in the column to place the temperature sensors. Also, when studying an existing

*Note to self, not part of thesis: expand on merits of fast temperature loop

column, the methods and procedures can still be used with a limited number of measurements. *

†

Available inputs

In the following analysis some limitations on the available manipulated variables u_2 have been assumed. The vapor split ratio, R_V, is excluded from the input set in all of the operational mode cases. Even though we have included R_V in the top-down analysis (Section 5.1), its practical implementation is still unresolved (See Chapter 10). Should a successful implementation of the vapor split as a manipulated variable be achieved it is still not likely to be used for regulatory control.

The vapor boil-up rate V is also omitted from the set of available inputs as it is a variable that is likely to saturate (evidently this is the case if nominally $V = V_{max}$ as in some of our cases). ‡

The set of available inputs then becomes:

$$\mathbf{u}_2^T = [R_L \quad L \quad S_1 \quad S_2] \tag{8.1}$$

8.3.1 Slope Criterion

We evaluate the temperature change from tray to tray in the column, and select for each of the four "profiles" to be stabilized the tray that experiences the largest temperature change. The temperature difference from one stage to the next can be seen in Figure 8.1. In the prefractionator, the tray above the feed is chosen, while in the top and bottom the trays just above and below the dividing wall have the largest slope. The middle tray in the middle main column section is the fourth temperature. In the notation of this thesis the stage numbers selected are:

$$T_{slope,1} = [T_{12} \quad T_{31} \quad T_{60} \quad T_{49}] \tag{8.2}$$

§ Minimize V in Figure 8.2

$$T_{slope,2} = [T_{12} \quad T_{31} \quad T_{61} \quad T_{52}] \tag{8.3}$$

*Note to self, not part of thesis: rephrase

†Note to self, not part of thesis: here have cut out older text that might be useful, saved in cutouts.txt

‡Note to self, not part of thesis: hmmm.. have used V in previous section.

§Note to self, not part of thesis: next part probably exclude but check slope for other cases.

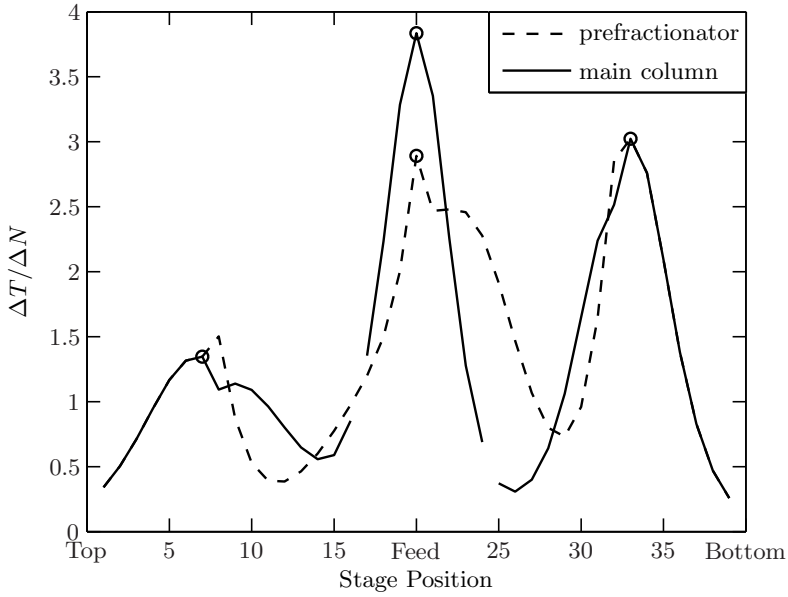

Figure 8.1: Case 1. Temperature difference from one stage to next, $T_{i+1}-T_i$. The chosen temperatures in each section are indicated.

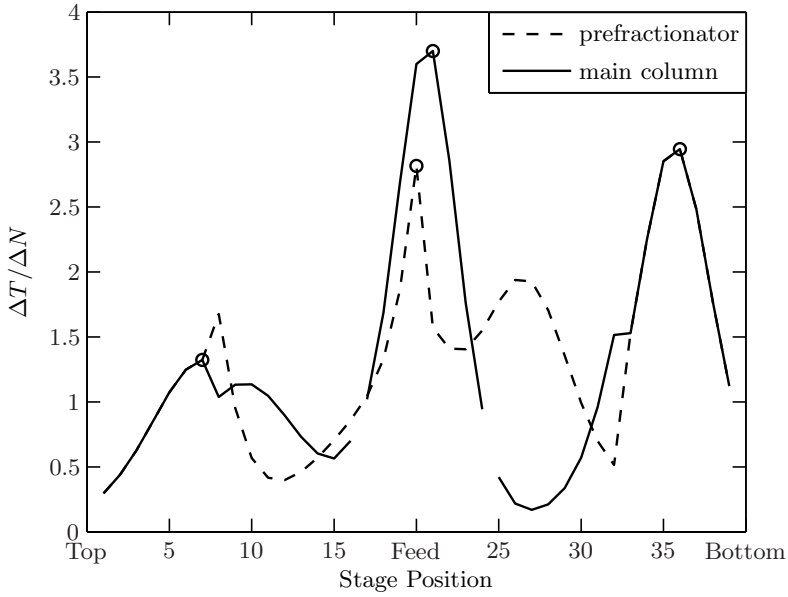

Figure 8.2: Case 2. Temperature difference from one stage to next, $T_{i+1}-T_i$. The chosen temperatures in each section are indicated.

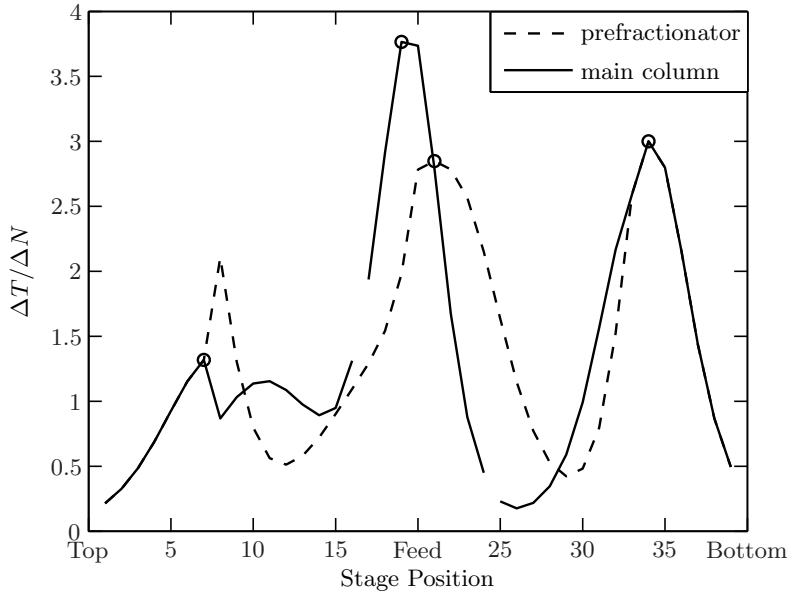

Figure 8.3: Case 4. Temperature difference from one stage to next, $T_{i+1}-T_i$. The chosen temperatures in each section are indicated.

Octanecase can be seen in Figure 8.3

$$T_{slope,3} = [T_{13} \quad T_{40} \quad T_{59} \quad T_{50}] \tag{8.4}$$

Max F exact same as min V.

8.3.2 Sensitivity criterion

The sensitvity criterion says that we should find the tray where there is the largest change in temperature for a change in manipulated variable. This is the same as maximizing the unscaled steady-state gain. The steady-state gains of the linearized model can be seen in figure 8.4. Again we decide to look for a temperature in each of the four main sections of the column. In doing this, we have already decided on the pairing of inputs to outputs, but any other pairing would lead to problems withinteractions. *

The four temperatures chosen from the sensitivity criterion are:

$$T_{sens,1} = [T_{17} \quad T_{33} \quad T_{61} \quad T_{50}] \tag{8.5}$$

*Note to self, not part of thesis: maybe more explanation needed here?

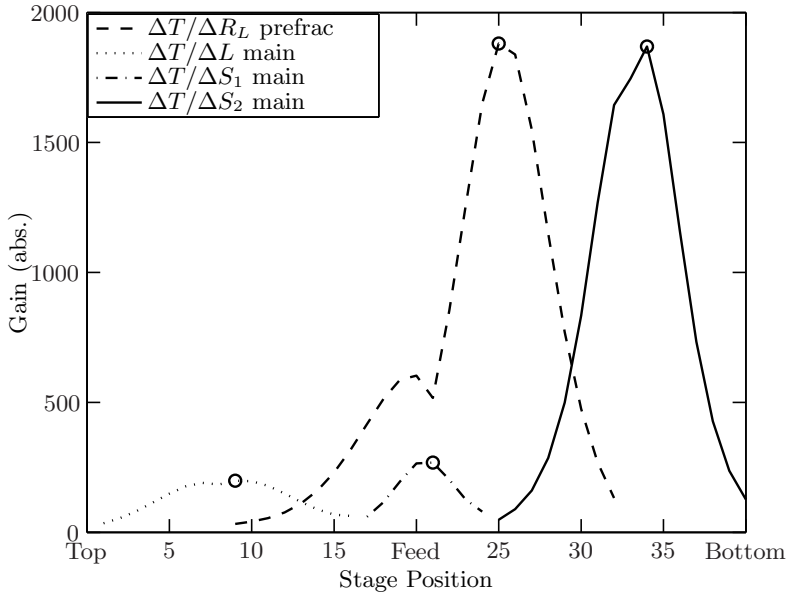

Figure 8.4: Steady-state gains of the column. Note that only the relevant input in each column part is shown along with the stage that has the maximum sensitivity.

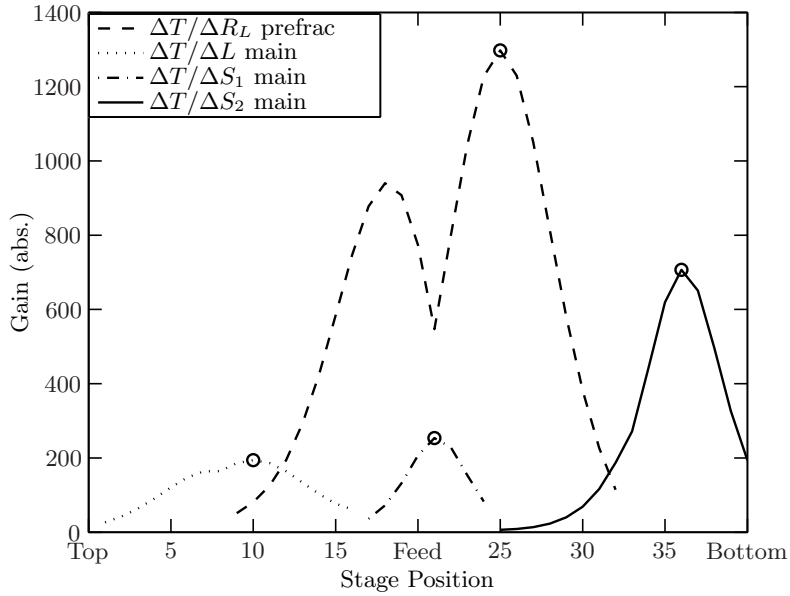

Figure 8.5: Steady-state gains of the column. Note that only the relevant input in each column part is shown along with the stage that has the maximum sensitivity.

Case min V. plot in Figure 8.5

$$T_{sens,2} = [T_{17} \quad T_{34} \quad T_{61} \quad T_{52}] \tag{8.6}$$

Case 3. plot in Figure 8.6

$$T_{sens,3} = [T_{15} \quad T_{35} \quad T_{60} \quad T_{51}] \tag{8.7}$$

Combined sensitivity and pair close

8.3.3 Maximum Gain Rule

Case 1. maximize purity

We return to Case 1 of Section 5.2.1 and the objective function in Equation 5.5. The linear model is now:

$$\Delta \mathbf{y}_{20} = \mathbf{G}^{y_{20}} \Delta \mathbf{u}_2 + \mathbf{G}_{d2}^{y_{20}} \Delta \mathbf{d}_2 \tag{8.8}$$

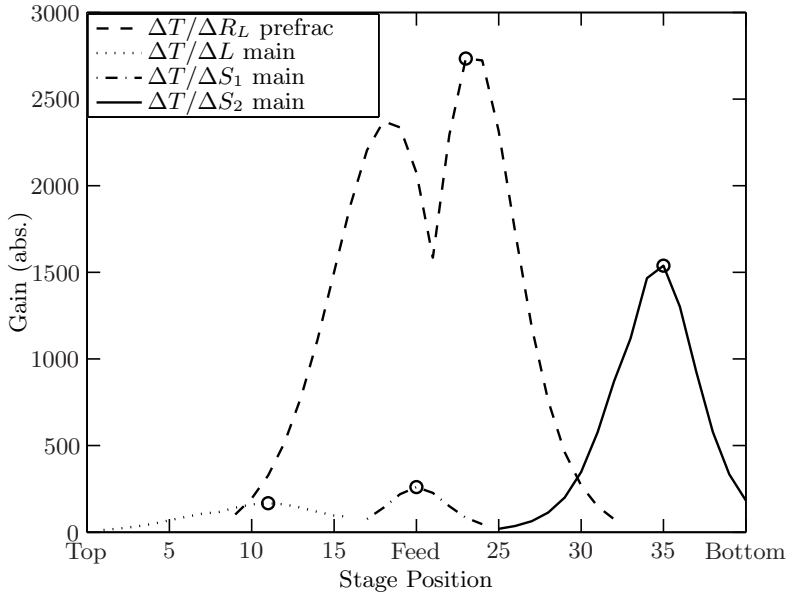

Figure 8.6: Steady-state gains of the column. Note that only the relevant input in each column part is shown along with the stage that has the maximum sensitivity.

Table 8.1: Temperatures for regulatory control

	R_L	L	S_1	S_2
Case 1				
Slope	T_{12}	T_{31}	T_{60}	T_{49}
Sensitivity	T_{17}	T_{33}	T_{61}	T_{50}
Max Gain	T_{13}	T_{38}	T_{58}	T_{49}
Case 2				
Slope	T_{12}	T_{31}	T_{61}	T_{52}
Sensitiviy	T_{17}	T_{34}	T_{61}	T_{52}
Max Gain				
Case 3				
Slope	T_{13}	T_{40}	T_{59}	T_{50}
Sensitivity	T_{15}	T_{35}	T_{60}	T_{51}
Max Gain	T_2	T_{57}	T_{41}	T_{55}

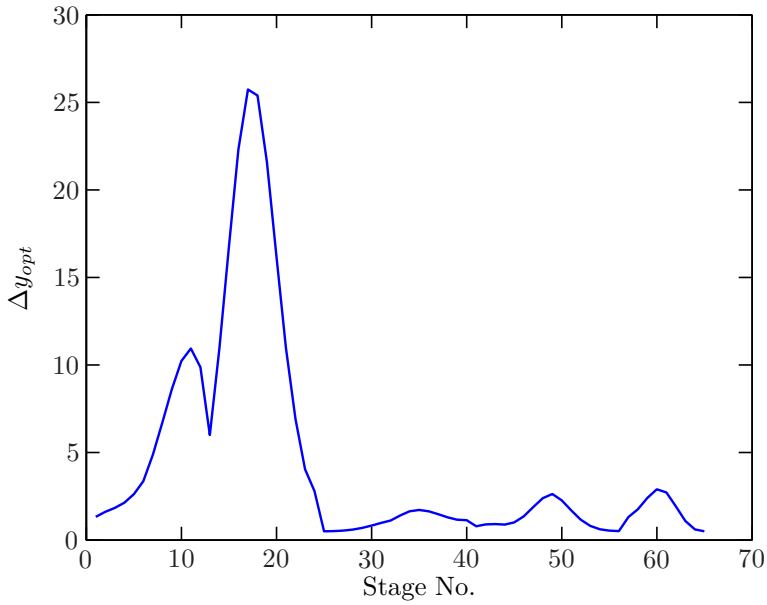

Figure 8.7: Optimal variation in outputs (span)

* where the disturbance vector includes V and R_V in addition to the feed conditions.

$$\mathbf{d}_2^T = [V \quad R_V \quad F \quad z_A \quad z_B \quad z_C \quad q] \tag{8.9}$$

The optimal variation for temperatures in the column can be seen in Figure 8.7. Note that the prefractionator comprises stages 1-24 and that the feed enters above stage 13. †

The scaled gain matrix, $\mathbf{G_s}$ is computed from Equation ‡.The scaled gains from the individual inputs can be seen in Figure 8.8.

Using the branch and bound algortihm by Cao [2] to find the maximum minimum singular value we get the best set of four temperatures to keep constant and the corresponding worst case loss. We denote the best set of controlled variables $\mathbf{y}_{2,G}$:

$$\mathbf{y}_{2,G}^T = [T_{13} \quad T_{49} \quad T_{38} \quad T_{58}] \tag{8.10}$$

The 10 best sets can be seen in Table 8.2. It can be noted that there is little difference in these sets. The feed stage (stage 13) is picked in all

*Note to self, not part of thesis: findbetter notation

†Note to self, not part of thesis: show figure for individual disturbances and comment

‡Note to self, not part of thesis: refer to equation in ch 2.

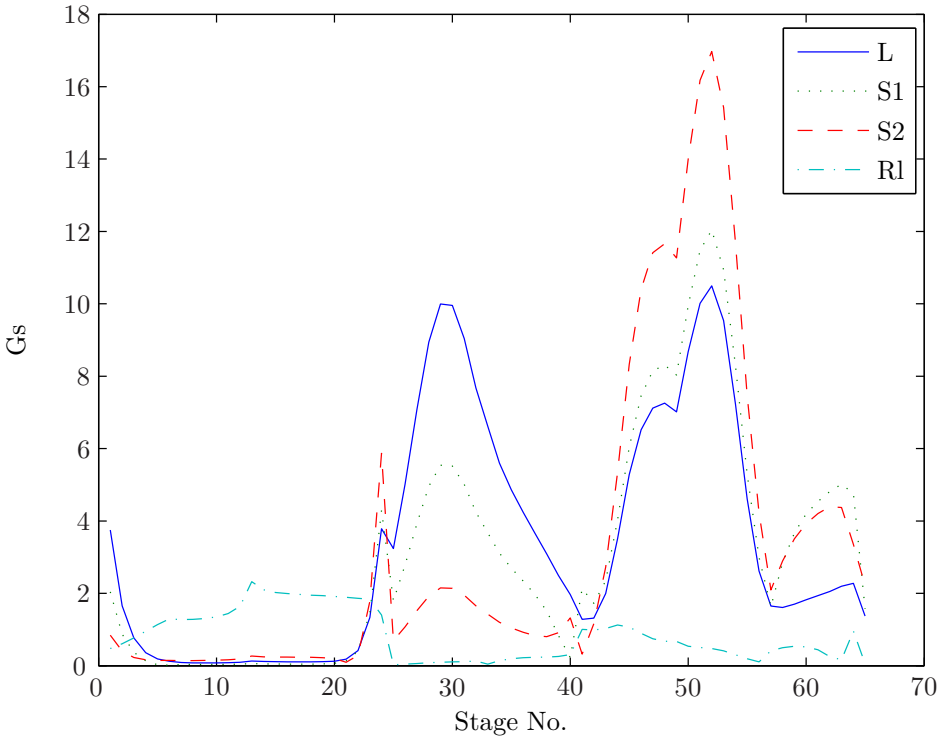

Figure 8.8: Scaled gains

Table 8.2: Sets of controlled temperatures

rank	stage no.				$\underline{\sigma}(\mathbf{G_s})$	loss
1	13	49	38	58	2.3409	0.0912
2	13	48	38	58	2.3409	0.0912
3	13	47	38	58	2.3409	0.0912
4	13	49	37	58	2.3409	0.0912
5	13	48	37	58	2.3409	0.0912
6	13	47	37	58	2.3409	0.0912
7	13	49	37	59	2.3408	0.0913
8	13	47	37	59	2.3408	0.0913
9	13	48	37	59	2.3408	0.0913
10	13	49	38	59	2.3408	0.0913

the best sets, as is a temperature around the lower end of the dividing wall (stage 47 just above, 48 and 49 just below). The third and fourth stages chosen are near the middle of column section 4 (stage 37 & 38) and towards the top of section 7 (stage 58 & 59).

The locations of the temperatures in the highest ranking controlled set can be seen in Figure 8.9a.

Loss using non-linear model

Using the same expected disturbances as in the linear analysis, we calculate the loss in the cost function using the non-linear model. The percentage loss can be seen in table 8.3.

Controllability

Pairing

We can use the rga of the reduced matrix G with the temperatures found in the highest ranking set to help us with pairing the inputs and outputs. ref. skogestad.We want to pair on rga-elements close to unitary. Alltough in this case it might seem intuitive to choose.

We see that we should pair R_l with the temperature in the prefractionator, and the others with... The control loops are indicated in figure 8.9b.

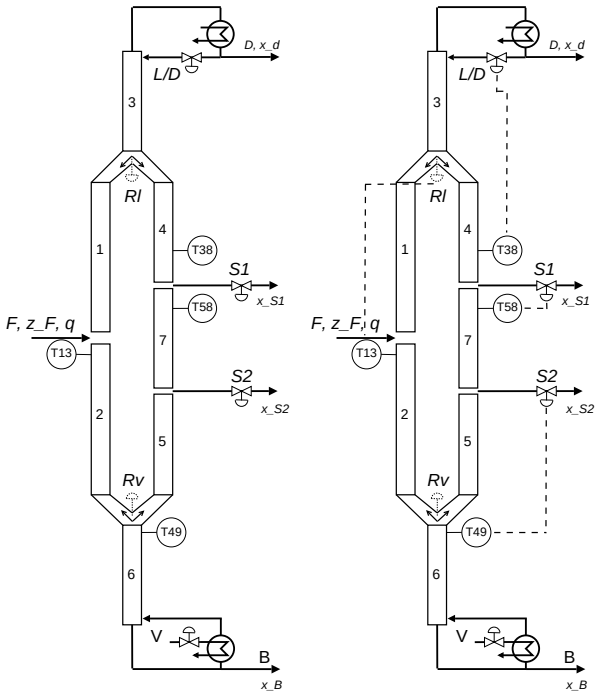

Figure 8.9: Controlled set CS 1

Table 8.3: Disturbance loss

disturbance	magnitude	%-loss
ΔV	$+10\%$	0.0016
ΔV	-10%	0.0092
ΔR_V	$+10\%$	0.0016
ΔR_V	-10%	0.0055
ΔF	$+10\%$	0.0070
ΔF	-10%	0.0184
$\Delta z_{A,F}$	$+5\%$	0.0042
$\Delta z_{A,F}$	-5%	0.0176
$\Delta z_{B,F}$	$+5\%$	0.0032
$\Delta z_{B,F}$	-5%	0.0178
$\Delta z_{C,F}$	$+5\%$	0.0001
$\Delta z_{C,F}$	-5%	0.0160
Δq	$+10\%$	0.0156
Δq	-10%	0.0237

Table 8.4:

	L	S_1	S_2	R_L
13	0.0012	-0.0171	0.0204	**0.9956**
49	0.0038	-0.0119	**1.0068**	0.0013
38	**1.0849**	-0.0905	0.0000	0.0056
58	-0.0899	**1.1196**	-0.0272	-0.0025

8.3.4 Case 2. Minimum Energy

The second mode of operation introduced (Section 5.2.2) was where we try to minimize the energy consumption of the separation subject to constraints on the product purities (Equation 5.6).

Maximum Gain Rule

Loss using non-linear model

Using the same expected disturbances as in the linear analysis, we calculate the loss in the cost function using the non-linear model.

Controllability

Pairing

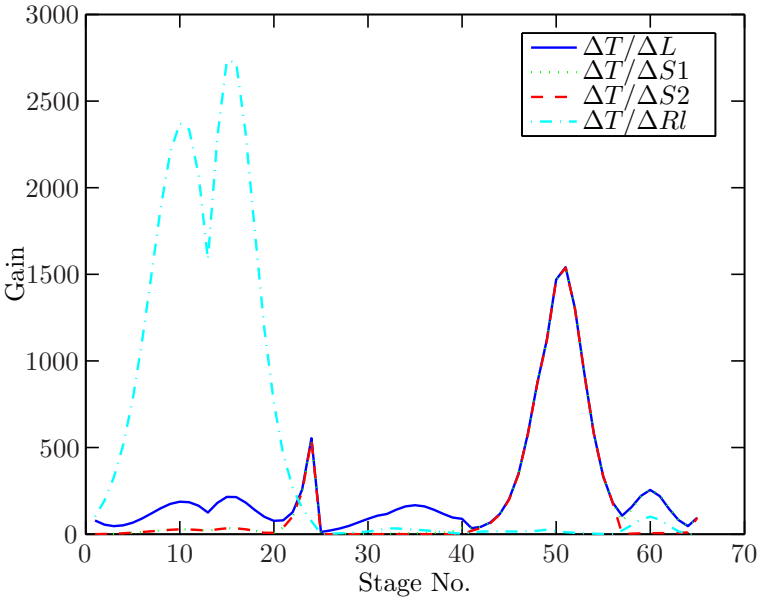

Figure 8.10: Steady-state gains

8.3.5 Case 4. Octane case

In Section 5.2.3 we described a case where only two of the products were of value.

Sensitivity criterion

The steady-state gains of the linearized model can be seen in figure 8.10.

Slope Criterion

Combined sensitivity and pair close

Maximum Gain Rule

Using the branch and bound algortihm by Cao .. to find the maximum minimum singular value we get the best set of four temperatures to keep constant and the corresponding worst case loss. The 50 best sets can be seen in table

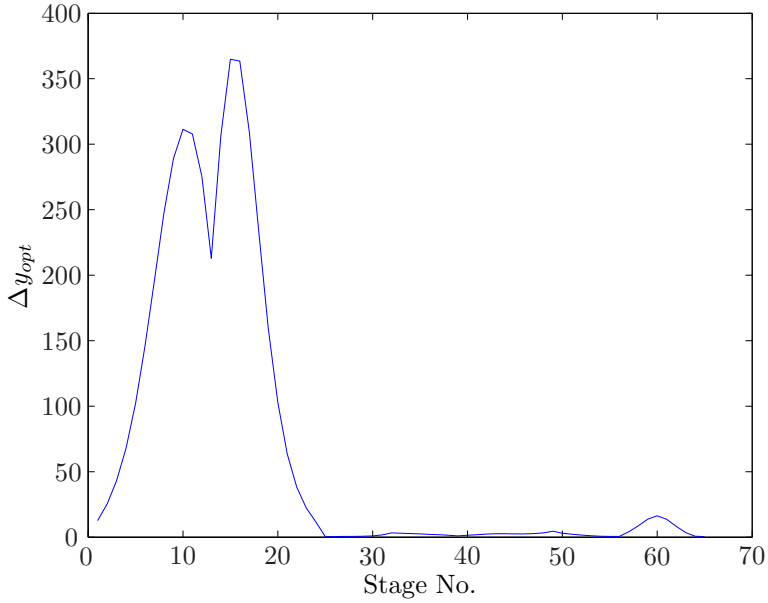

Figure 8.11: Optimal variation in outputs (span)

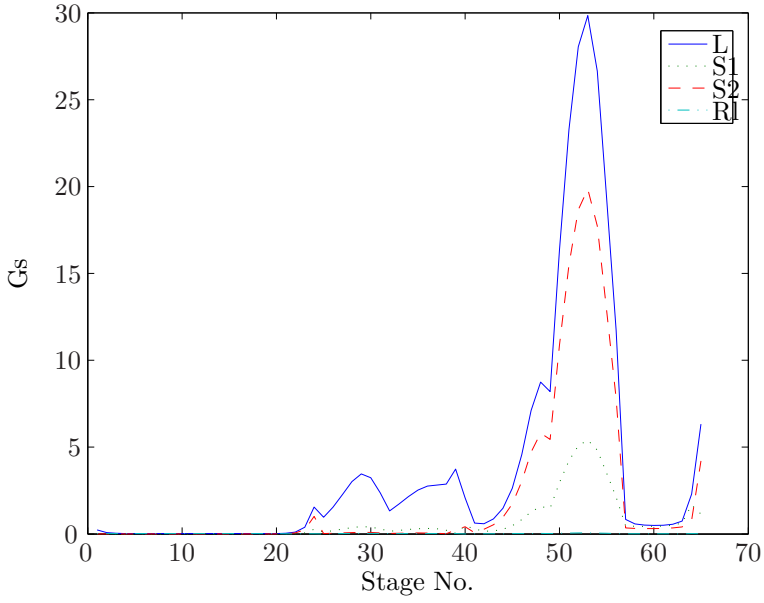

Figure 8.12: Scaled gains

Table 8.5: Sets of controlled temperatures

rank	stage no.				min sv	loss
1	41	2	57	55	0.0282	627.0426
2	41	2	57	54	0.0282	627.0993
3	41	2	57	56	0.0282	627.1027
4	41	2	57	53	0.0282	627.2678
5	41	2	57	65	0.0282	627.4816
6	41	2	57	52	0.0282	627.6539
7	41	2	51	57	0.0282	628.5918
8	41	2	50	57	0.0281	631.1930
9	41	2	48	57	0.0280	639.2996
10	41	2	49	57	0.0280	639.7366

Loss using non-linear model

Using the same expected disturbances as in the linear analysis, we calculate the loss in the cost function using the non-linear model.

Controllability

Pairing

	L	S_1	S_2	R_L
41	-3.7235	**5.4080**	-1.0203	0.3358
2	0.4574	0.0073	-0.0048	**0.5401**
57	**2.2067**	-1.3292	-0.0047	0.1272
55	2.0594	-3.0862	**2.0299**	-0.0031

We see that we should pair R_L with the temperature in the prefractionator, and the others with... The control loops are indicated in figure 8.13b.

8.3.6 sets assuming J_{uu} unitary

*

*Note to self, not part of thesis: Use simple scaling of inputs. what is the difference

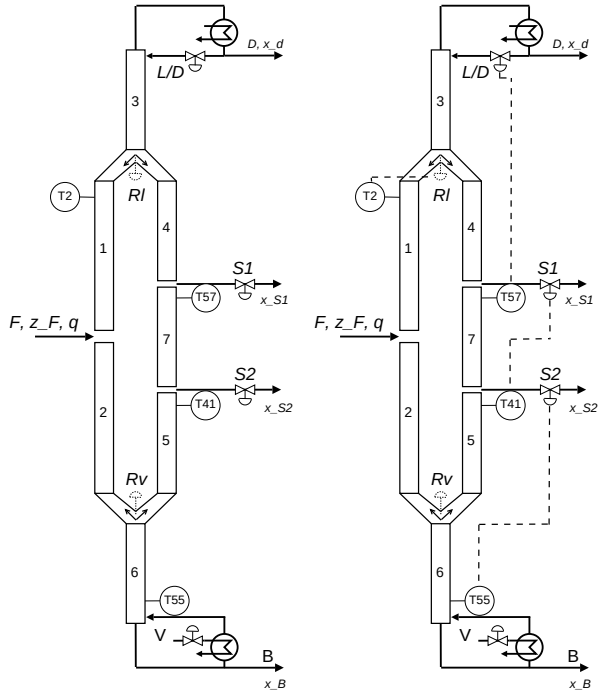

Figure 8.13: Controlled set CS 1

Table 8.6: Sets of controlled temperatures

rank	stage no.				min sv	loss
1	64	32	40	55	8.9629	0.0062
2	64	32	40	56	8.9627	0.0062
3	64	32	40	54	8.9625	0.0062
4	64	32	40	53	8.9613	0.0062
5	64	32	40	65	8.9607	0.0062
6	64	32	40	52	8.9586	0.0062
7	64	32	40	51	8.9521	0.0062
8	64	32	40	50	8.9339	0.0063
9	64	32	48	40	8.8767	0.0063
10	64	32	40	49	8.8737	0.0063

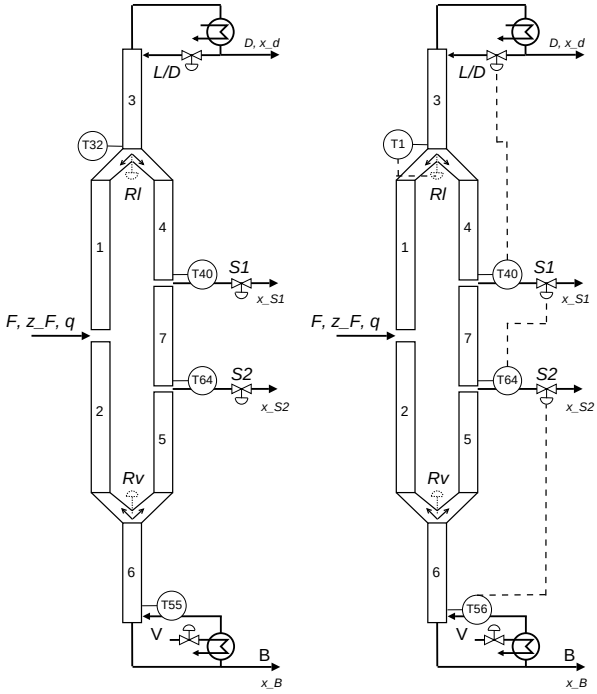

Figure 8.14: Controlled set CS 1

Pairing

	L	S_1	S_2	R_L
64	-0.6931	**1.8925**	-0.2775	0.0781
32	0.2064	-0.0096	-0.0001	**0.8032**
40	**1.3354**	-0.4556	-0.0011	0.1212
55	0.1513	-0.4274	**1.2787**	-0.0026

We see that we should pair R_L with the temperature in the prefractionator, and the others with... The control loops are indicated in figure 8.14b.

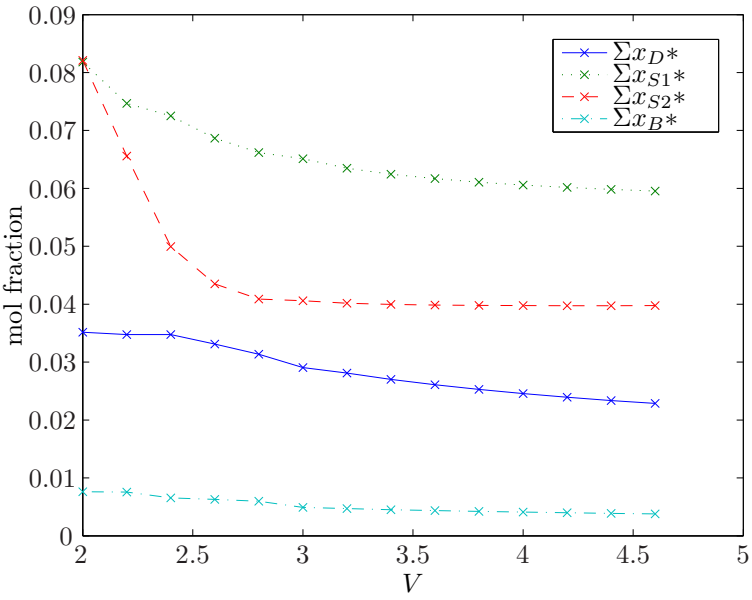

Figure 8.15: sum of impurities in each product stream

8.4 Dynamic simulations

8.4.1 Case 1 - additional investigations

*

Sum of the impurity stream as a function of vapour boilup can be seen in figure 8.15. The optimal value of the sum of all impurity flows can be seen in figure 8.16.

Now we close the 4 loops with the pairing found earlier and see how the how the objective function behaves with vapour boilup, V, as a disturbance. In figure 8.17 we see the individual product stream impurities, and in figure 8.18 the objective function is plotted against V.

*Note to self, not part of thesis: where to put this?

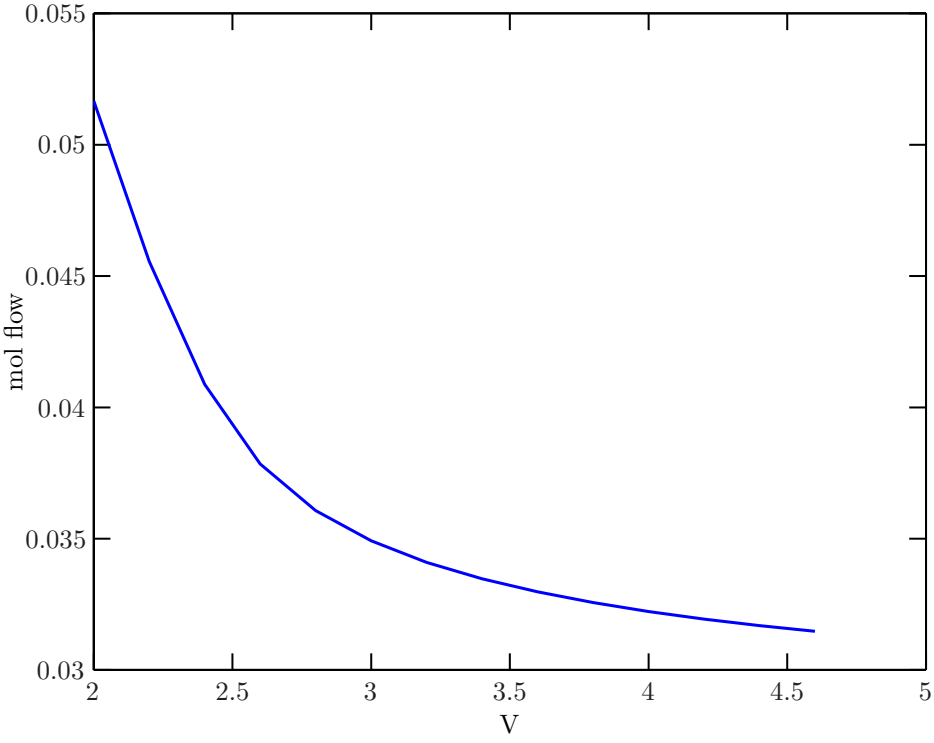

Figure 8.16: Minimum impurity flow as a function of vapour boilup

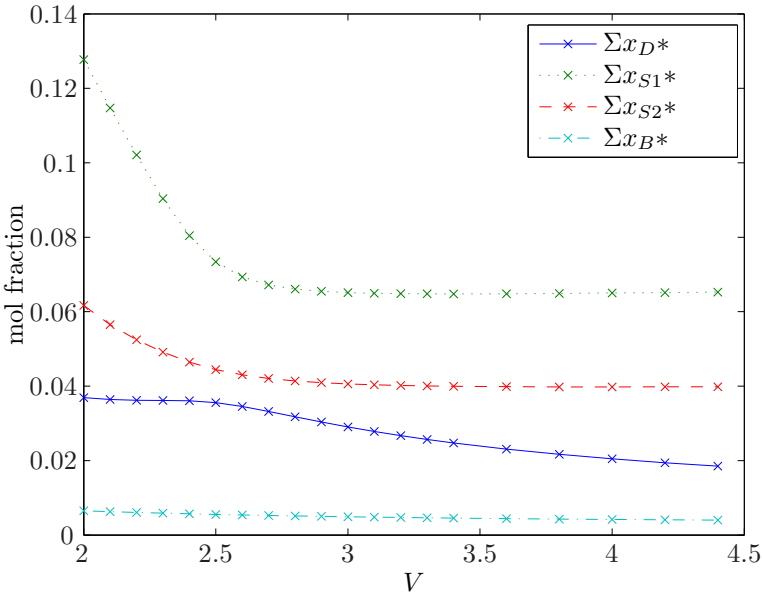

Figure 8.17: Closed loop: sum of impurities in each product stream

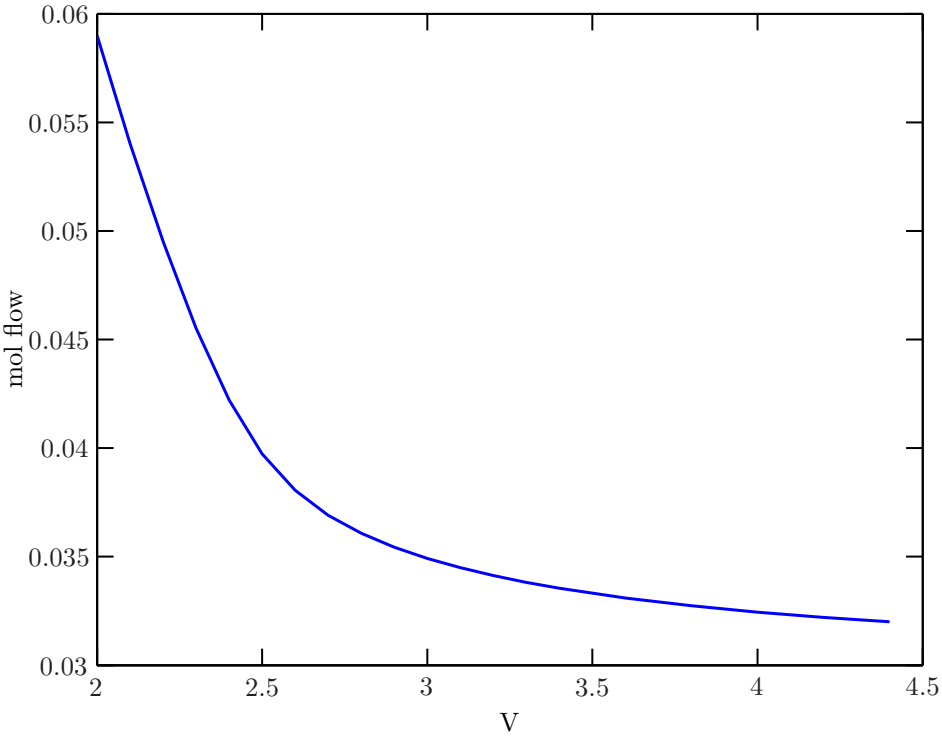

Figure 8.18: Closed loop: sum of impurities in each product stream

Chapter 9

Experimental Column

9.1 Introduction

The laboratory Kaibel distillation column was built with the purpose to study its practical operation and control. Wheras experimental results from pilot plant versions of the Petlyuk column or equivalent three-product dividing-wall columns are available*, results from experimental work on the 4-product Kaibel column has not been published to date. It is, however, known that BASF are operating a few Kaibel dividing-wall columns (and have also experimental facilities.)†

The design chosen for the column was not a dividing-wall column but rather a thermodynamically equivalent two-shell realization of the fully thermally-coupled column. The choice was made because it was believed that a two-shell column is easier to build and operate in practice. In addition, the department already had a number of spare glassware column sections.

9.2 The column

The Kaibel column is built in the Experimental Hall at the Chemical Engineering department. It is supported by an aluminium frame as shown in Figure 9.1. The column itself is made of glass sections produced by Normag Labortechnik in Germany. The standard sections have an inner diameter of 50 mm. They are vaccuum jacketed so that the flange size is DN 80. The outer jacket wall has a silver coating to reduce radiation loss, but sight-strips

*Note to self, not part of thesis: quote references
†Note to self, not part of thesis: find reference

are included to allow some inspection into the inner column. The standard column sections used are 900 and 730 mm respectively, while the liquid-divider sections (product draws) are 450 mm in length. The "splitting" sections that combine prefractionator and main column shells are custom made into Y-shapes of approximately 500 mm length. The liquid dividers and feed sections have threaded connections (GL25) for product and feed tube attachment. Those parts as well as the Y -sections have extra connections used for inserting temperature sensors inside the column.

The liquid-dividers

The dividers facillitates the liquid draw off via a swinging funnel operated with a solenoid magnet (Fig. 9.2). At the top of the section is a type of tray that collects liquid into a downcomer. The downcomer leads the liquid into the swinging funnel, and depending on its posistion the liquid will either continue down the column as reflux or it will be led into a side pocket and drawn off as product.

column connectors

* The top Y-piece or splitting section also has a swinging funnel incorporated for the distribution of liquid to the two columns. Here, a wall is positioned directly below the funnel outlet and the funnel swings to either side of the wall.

Vapor-split valves

The original valves installed were butterfly-valves in stainless steel. The flanges were equal to the ones on the glass column sections but to avoid excessive weight, the inner diameter were kept at 80 mm (the normal diameter for a DN 80 flange as there is no double wall here as opposed to the glass sections). The valves had a manual handle with a 90 degree range between fully open and fully closed.

Reboiler

The reboiler is a kettle type boiler made of stainless steel and has a maximum capacity of approximately 15 litres. Electrical heating elements with a combined effect of 3 kW are inserted through the wall near the bottom of the tank. The minimum liquid volume required to cover the elements is 3

*Note to self, not part of thesis: rewrite!

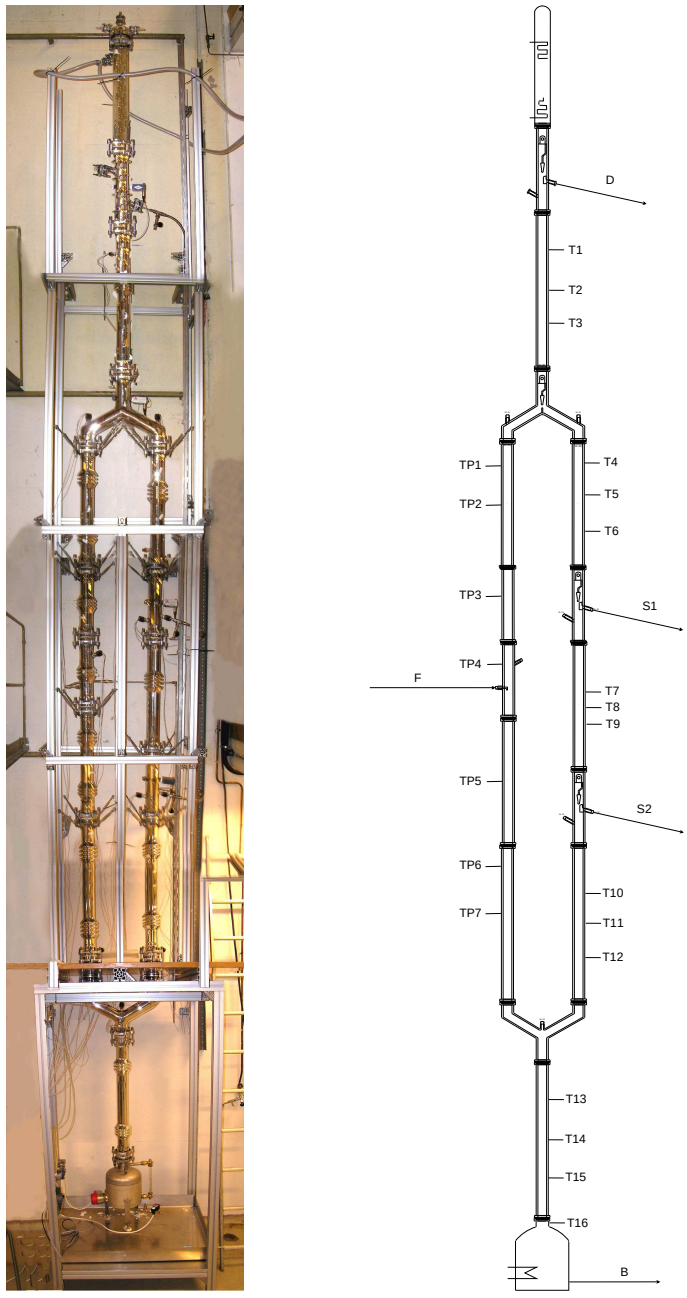

(a) (b)

Figure 9.1: Laboratory Kaibel column. (a) Assembled photo showing column and supporting frame. (b) Scaled drawing indicating streams and the locations of temperature sensors.

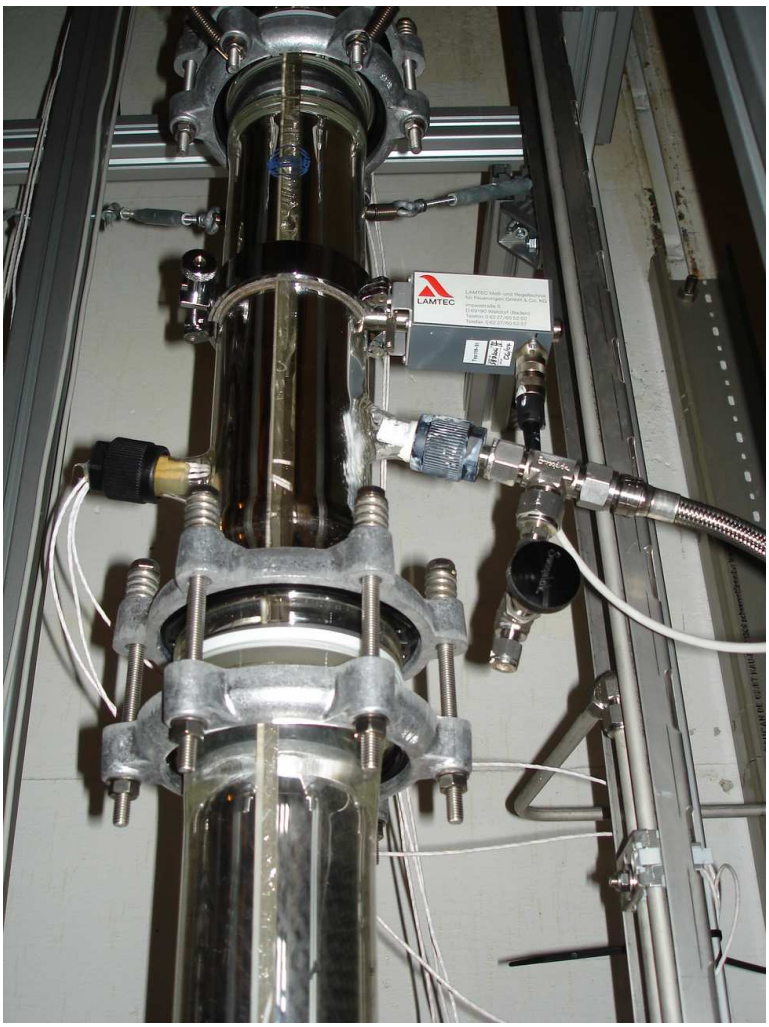

Figure 9.2: Sidestream product draw. Swinging funnel inside column section directs the liquid to the product line or as reflux.

litres. A sightglass is attached to the side of the reboiler to allow for manual monitoring of the liquid level.

Condenser

The condenser sits directly on top of the column as a further extension to the topmost column section. There is no distillate/reflux tank from which the reflux is drawn, instead the condensed liquid flows back down, countercurrent to the vapor, and into the swinging funnel that directs the liquid to either distillate product or reflux. The swinging funnel thus sets the L/D ratio of flows.

Packing

To facilitate the placement of temperature sensors inside the column sections, it was decided to fill the column with random packing material. For cost effectiveness and simplicity, Glass Raschig rings with a diameter of 6 mm was used.

9.3 Mounting of the column

The column is built inside and supported by an aliminium frame. Because the stainless steel valves were rather heavy and they were to be mounted directly atop the bottom Y-piece it was decided that the valves had to be fixed to the mounting frame and thus become the fixation point of the whole column. This is mainly to protect the glass Y-piece from excessive stress from the weight of the valves but also to prohibit the movement of the valves when operating the handles. The fixed point of the column was then about 2 metres above "ground level", with the sections below the valves hanging free. The weight of the reboiler is compensated with springs attached to the column frame. Above the valves, the column sections are resting on top of each other but their weight is also compensated using springs. 4 springs and adjustable turnbuckles are attached to each flange-connection. The springs are adjusted to lift the weight of the section below. The spring system has a dual effect; while lightening the pressure on the glass section it also helps in positioning the column.

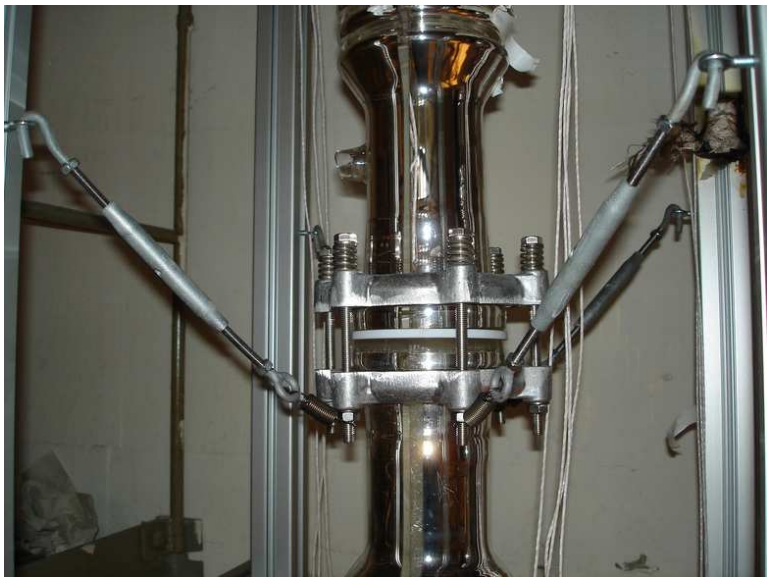

Figure 9.3: Springs and turnbuckles help centering the column and relieves pressure from the sections below

9.4 Instrumentation

Measurements

Inside the column, a total of 24 temperature sensors of type PT-100 are placed at various locations. The individual sensors with wire are inserted in the relevant column section during the filling of the Raschig rings, so that the packing keeps the sensors in place. In addition to the PT-100 elements, thermocouples (type K) are used for external temperature measurements on heating tapes, feed tube and reboiler wall etc.

The only other measurement available is a differential pressure sensor, used to monitor the liquid level in the reboiler.

Inputs

* The feed is pumped and metered by a diaphragm pump. The speed is set remotely from the control interface. The bottoms product draw is controlled using a solenoid valve. The three other product draws plus the liquid split divider are all operated by swinging funnels. They act as on-off valves and are controlled using solenoids attached to the outside of the column wall.

*Note to self, not part of thesis: find better name

9.5 Data aquisition and control

All the measurements and actuators are connected to a Fieldpoint modular I/O system from National Instruments in a central cabinet. The system consists of several interconnected Fieldpoint modules that are either input or output modules. A network interface module, FP-1000, connects the modules to a PC through an RS-232 cable. The PT-100 elements are connencted to three modules of type FP-RTD-124 while the pressure measurement is connected to an analog input module of type FP-AI-112. An FP-TC-120 connects the thermocouples. The actuators are connected via two FP-AO-200 analog output modules. The analog output modules deliver current output in the range 4-20 mA, and *

9.5.1 Labview interface

The column is operated using an interface (Figure 9.4) created in the LabVIEW development tool from National Instruments. It is the interface that reads and writes the signals to the Fieldpoint interface module. Measurements are visualized on the computer screen an the values of the actuator can be manipulated. All measurement and actuator signals are also written and stored to a data file during an experiment. The LabVIEW interface also includes the various controllers used in the column operation.

Controllers

There are four PID-controllers implemented through the LabVIEW interface. These are temperature loops used for keeping selected temperature measurements at various positions in the column constant. The actuators are the four swinging funnels that operate in a timed cycle. The swinging funnels have two positions: The position “at rest” is the default position when no current is sent to the solenoid. The funnel hangs vertically straight down and the liquid continues down the column. In the case of the liquid split the liquid is sent to the prefractionator side of the column partition. At the “excited” position, the solenoid is activated an the funnel swings towards the column wall sending the liquid into the product line, or, in the case of the liquid split sends the liquid to the main column side of the partition. A fixed interval of 5 seconds is used, during which the funnel will swing between its end positions at most once each way. The manipulated variable is the ratio of the time that the funnel spends in the rested position to the total time of the cycle (5 seconds). Assuming that the liquid flow

*Note to self, not part of thesis: snakk med A Fjellviks for info

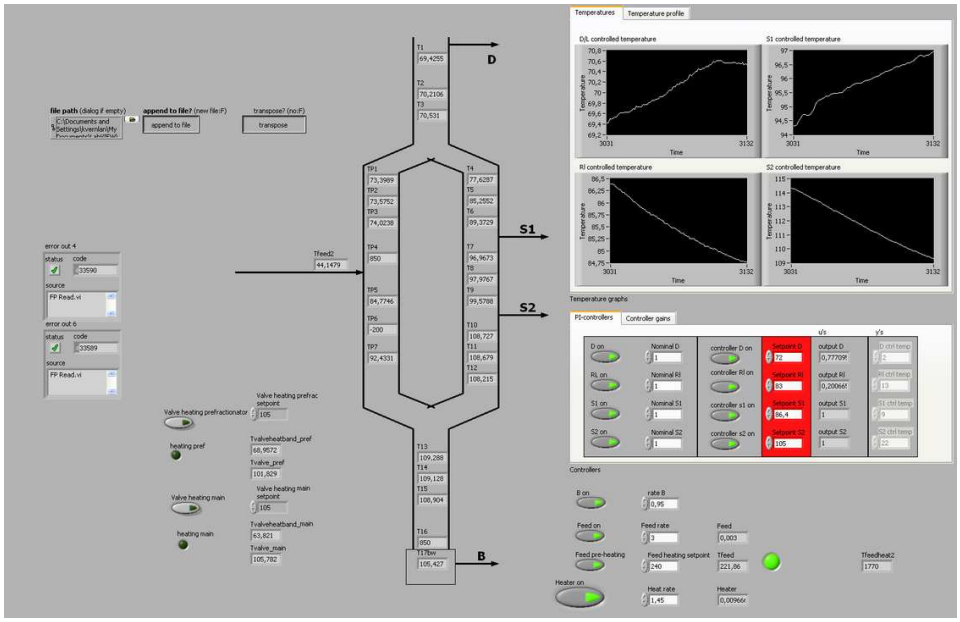

Figure 9.4: Graphical user interface for the column operation

rate into the funnel is constant during this interval, we can then describe the manipulated variable as the ratio of reflux to the total liquid into the funnel. E.g. for the funnel controlling the distillate product we have:

$$u_D = \frac{L}{L+D} \qquad u_D \in [0,1] \tag{9.1}$$

Thus, for a value of $u_D = 1$ we have total reflux, while a value of $u_D = 0.8$ means that the funnel will move to the side of the wall for one second, then move back to the resting position and remain there for four seconds. The other product draws are defined similarly, while for the liquid split the input is defined as:

$$R_L = u_{R_L} = \frac{L_p}{L_p + L_m} \qquad R_L \in [0,1] \tag{9.2}$$

where L_p and L_m is the liquid flowing to the prefractionator side and main column side of the partition respectively.

The control algorithm used is one of LabVIEW's PID controllers (PID Advanced.vi) with bumpless transfer and anti wind-up. Only proportional and integral action have been used.

A part from the PID loops, the heating tapes on the feedline and vapor split valves are controlled using thermostat control.

Chapter 10

Experiments

10.1 Introduction

The Kaibel Columm experimental rig was built for the purpose of studying the operation and control of the column.

The experimental work so far ..

10.2 experiments

10.2.1 controller tuning

10.2.2 model verification?

10.2.3 effect of liquid split

10.2.4 manipulating vapor split

Dividing-wall columns, and most thermally coupled columns, have one feature that distinctly separates it from conventional distillation columns. That is the distribution of liquid and vapor flows to the different column partitions. For a dividing-wall column with the partitioning wall vertically positioned in the middle of the column (ie. there are column sections above and below the wall), we have what we denote a liquid split at the top of the partition and a vapor split at the bottom. A suitable ratio of flows to either side of the partition is very important to the successful operation of a dividing-wall column.

The industrial dividing-wall columns will have some type of device for the liquid split and a couple of solutions have been reported. CAN PUT REFERENCES HERE. A liquid spliiting device can be incorporated into

a special tray with a liquid holdup. The liquid can be distributed to the desired side by gravity alone which is a great advantage. Though it is not known whether the industrial columns use the liquid split actively in feedback control, we have shown earlier that this can be very beneficial and in some cases crucial to achieving optimal operation.

In the case of the vapor split the situation is quite different. There are no reports of adjustable vapor splits in the literature, nor has it been reported by the industrial ... Montz REF has a been successful in implementing a moveable wall that can be adjusted sideways so as to increase/decrease the relative volume available either side of the wall. This can be adjusted during the commissioning of the column, but once the column is up and running the wall is fixed. Usually the detailed design will determine the best position of the wall and the pressure drop either side of the partitioning will determine the vapor split ratio. One can argue that if the desired vapor split ratio is not achieved it can be compensated by adjusting the liquid split. This is true up to a point as we have shown in Chapter REF KAIB VV PET, but if the ratio is too far off from the optimal value the product purities or at least the column efficiency will suffer. It would therefore be of great advantage to the operation of a dividing-wall column, be it with one or more side streams, to be able to adjust the ratio of vapor flows during operation. This is certainly the case if the column is subject to frequent changes in the feed as the optimal settings of both vapor and liquid split ratios will move with varying conditions. If, in addition, a method of adjusting the vapor split was found that was relatively fast and could be manipulated automatically, one would have an extra degree of freedom for control that could be used to increase purities or make the separation more energy efficient in the face of process disturbances.

butterfly valves

The thought of achieving the vapor split was present when the decision to build a pilot of the Kaibel column was taken. Though, in hindsight it must be admitted that the earliest attempts were made (without a great deal of thought)*... Nevertheless, when the column was built, two butterfly valves were installed in parallel above the section that forks the bottom column section into the two separate "columns" of the prefractionator and main column (Fig. 10.1) . The valves were with a large bore of almost 80 mm diameter (as compared to 50 mm i.d of the column sections. This was to allow connection to the column sections which has flanges of DN 80), and

*Note to self, not part of thesis: skriv om dette!

Figure 10.1: First valves installed for the adjustment of the vapor split.

were controlled manually using levers.

The large size of the valves were ultimately their biggest drawback. When going from a fully open position to fully closed, there were no observable redirection of the vapor flow until the valve was virtually closed. The only available measurements from which to deduce changes in the internal flows were the temperature sensors, but they should give a clear indication if a change in R_V has occured. The large diameter of the valve meant that even with only a small opening there were sufficient total are for the flows not to cause significant change in the pressure drop across the valve. Fine adjustment of the valve position was also difficult with the manual levers.

-Show plot from experiment here! (maybe)

air-water rig

The experience of the butterfly valves showed that it would be difficult to adjust the vapor flow by constraining the entire cross-section of the column. A method where one could manipulate only the vapor flow after first separating the vapor from the liquid seemed more feasible. This would be analogous to the way the liquid split is performed. A crude experimental rig was set up to test some new ideas for a valve design (Figure 10.2. To separate liquid from vapor it was decided to collect the liquid on a tray

new valves

With the new vapor split valves installed, some experiments have been performed that show some promise. Whereas adjusting the butterfly valves in practice led to only two valve positions, fully open or fully closed, the new valves can be adjusted to achieve varying vapor flow.

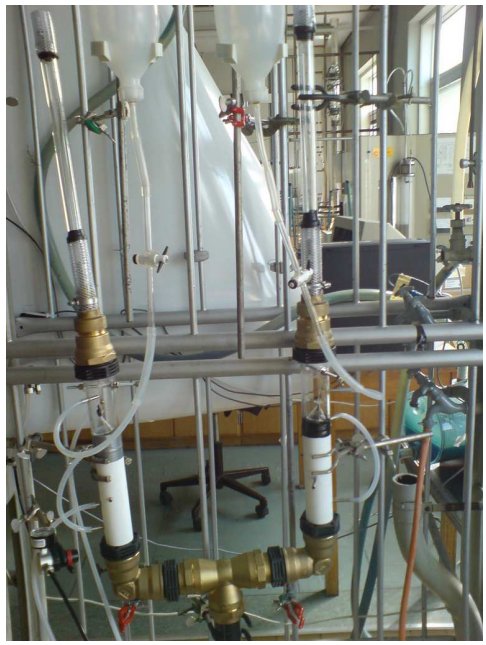

Figure 10.2: Rig for testing new valve solutions using air and water

Figure 10.3 shows the temperature responses for the measurements on the main column side (Fig 10.3a) and prefractionator side (Fig 10.3b) respectively. At time $t = 18700$ s the valve on the main column side is moved towards closing, and at $t = 21300$ s the valve is further closed. We notice that the temperatures in the prefractionator (Fig 10.3b) are increased, indicating that more vapor is being led into these sections. The temperatures below the second sidestream (S_2) are also increased, which can be explained by the decrease in lighter components coming down the prefractionator. Further up the main column the temperatures are decreased due to the lowered vapor rate. These effects are confirmed by simulations as resulting from a positive change in R_V, ie. more vapor is sent to the prefractionator. The change could also be observed from the measured pressure drop across the manipulated valve. With the valve in the open position ($t <$ 18700 s) the manometer reading showed a pressure drop of $\Delta P = 8$ mm H_2O. After the first step, the pressure drop increased to 10 mm H_2O and the second step gave a pressure drop of 12 mm H_2O. Figure 10.4 shows how the column temperature profile changes as a result of the steps in R_V. The profiles are shown for time instances before the first step is made (Fig 10.4a), just before the second step (10.4b) and some time after the second

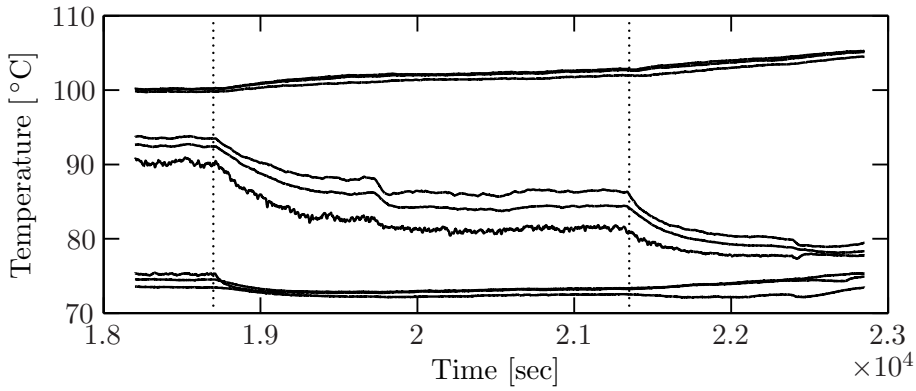

(a) Temperatures on main column side of partition

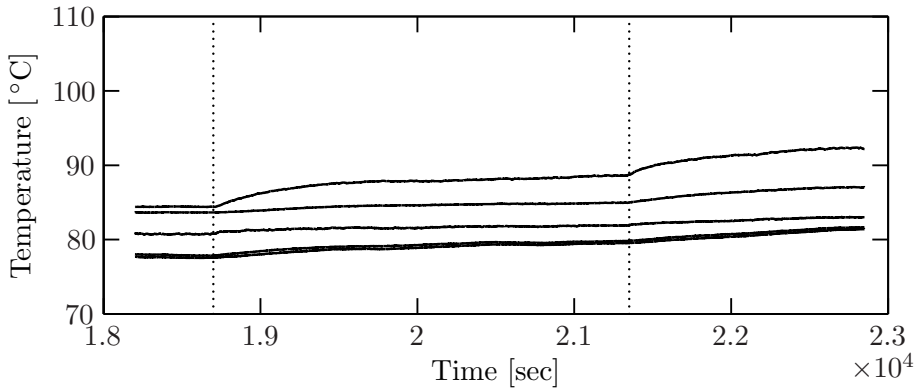

(b) Temperatures on prefractionator side of partition

Figure 10.3: Temperature responses to change in R_V

step (10.4c). One can clearly see how the middle part of the main column is cooled causing a marked shift in the column temperature profile.

During this experiment, the controllers were set to manual, with the exception of L which was used to control a temperature (T_3) in the top section. After the steps in R_V, this controller eventually saturated and gave close to total reflux in the top. The rates of R_L, u_{S_1} and u_{S_2} were set at 0.3, 0.8 and 0.8 respectively.

10.2.5 discussion vapor split

The experiment with the new vapor split valves show that it is possible to manipulate the vapor flow at least to some extent. With reliable measure-

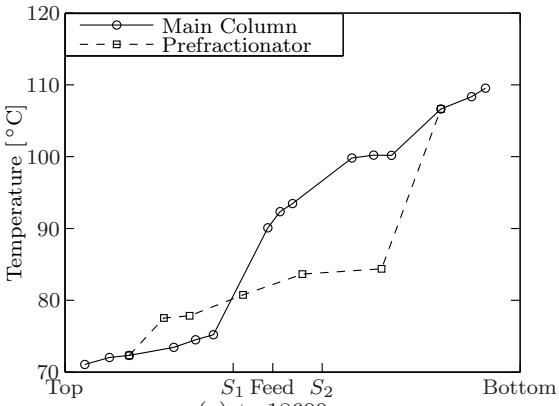

(a) t=18600 s

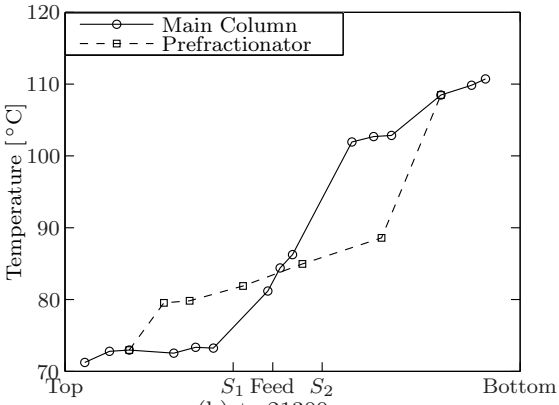

(b) t=21300 s

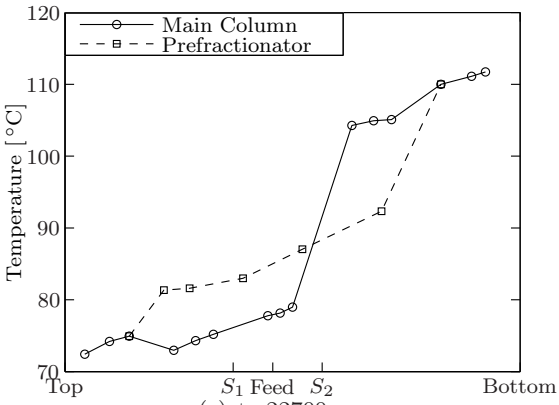

(c) t=22700 s

Figure 10.4: Shift in temperature profile after change in R_V. Valve on main column side is closed in two steps. The marked points are represent the measurements and the lines are only for visualization.

ments of the pressure drop across the valves it would also be possible to adjust the valves online with a constant setpoint on the pressure drop for one of the valves for example. The present valve design is probably not suited for online control, however. The range of valve positions in which adjustment has an observable effect is still very limited. Over the full range of positions from fully open to fully closed, more than 95 % of the span is effectively a fully open valve position. With the current step motor this translates to less than 10 half-steps available for real adjustment and a controller would spend most of its time saturated. * Resizing the gear system could improve the available input range and make feedback control easier, (but a more thorough redesign of the valve is probably needed for the full range of R_V to be available.†) For industrial scale applications this type of valve would of course be impractical, but we believe that the method presented here where the liquid and vapor are separated before adjusting the vapor flow could form the basis for a solution that could also be implemented on a larger scale.

Given a functioning valve adjusted online to control the pressure drop across it, as described above, there still remains the question of what setpoint to use to achieve the correct (or optimal) vapor split for the column. We would probably need some other measurement than the differential pressure over one or both valves to determine the R_V split ratio. Here

*Note to self, not part of thesis: riktig?
†Note to self, not part of thesis: maybe cut this

Bibliography

[1] V. Alstad. *Studies on Selection of Controlled Variables*. PhD thesis, NTNU, 2005.

[2] Y. Cao and P. Saha. Improved branch and bound method for control structure screening. *Chem. Engng. Sci.*, 60:1555–1564, 2005.

[3] I. J. Halvorsen, S. Skogestad, J. C. Morud, and V. Alstad. Optimal selection of controlled variables. *INDUSTRIAL & ENGINEERING CHEMISTRY RESEARCH*, 42(14):3273–3284, 2003.

[4] I.J. Halvorsen and S. Skogestad. Optimal operation of petlyuk distillation: A steady-state behavior. *J. of Process Control, Special issue: Selected Papers from Symposium PSE-ESCAPE '97, Trondheim. Norway, May 1997*, 9(5):407–424, 1999.

[5] S. Skogestad. The dos and don'ts of distillation columns control. *Chemical Engineering Research and Design (Trans IChemE, Part A)*, 85(A1):13–23, 2007.

[6] A. C. Vosloo. Fischer-tropsch: a futuristic view. *FUEL PROCESSING TECHNOLOGY*, 71(1-3):149–155, 2001.